Quaternary Science Reviews 180 (2018) 240–259

Contents lists available at ScienceDirect

Quaternary Science Reviews

journal homepage: www.elsevier.com/locate/quascirev

New age constraints for the Saalian glaciation in northern central Europe: Implications for the extent of ice sheets and related proglacial lake systems

Jörg Lang [a, *], Tobias Lauer [b], Jutta Winsemann [a]

[a] Institut für Geologie, Leibniz Universität Hannover, Callinstraße 30, 30167 Hannover, Germany
[b] Department of Human Evolution, Max Planck Institute for Evolutionary Anthropology, Deutscher Platz 6, 04103 Leipzig, Germany

ARTICLE INFO

Article history:
Received 19 June 2017
Received in revised form
14 November 2017
Accepted 21 November 2017

Keywords:
Middle Pleistocene
Saalian glaciation
Ice-dammed lake
Lake-outburst flood
Luminescence dating

ABSTRACT

A comprehensive palaeogeographic reconstruction of ice sheets and related proglacial lake systems for the older Saalian glaciation in northern central Europe is presented, which is based on the integration of palaeo-ice flow data, till provenance, facies analysis, geomorphology and new luminescence ages of ice-marginal deposits. Three major ice advances with different ice-advance directions and source areas are indicated by palaeo-ice flow directions and till provenance. The first ice advance was characterised by a southwards directed ice flow and a dominance of clasts derived from southern Sweden. The second ice advance was initially characterised by an ice flow towards the southwest. Clasts are mainly derived from southern and central Sweden. The latest stage in the study area (third ice advance) was characterised by ice streaming (Hondsrug ice stream) in the west and a re-advance in the east. Clasts of this stage are mainly derived from eastern Fennoscandia. Numerical ages for the first ice advance are sparse, but may indicate a correlation with MIS 8 or early MIS 6. New $pIRIR_{290}$ luminescence ages of ice-marginal deposits attributed to the second ice advance range from 175 ± 10 to 156 ± 24 ka and correlate with MIS 6.

The ice sheets repeatedly blocked the main river-drainage pathways and led to the formation of extensive ice-dammed lakes. The formation of proglacial lakes was mainly controlled by ice-damming of river valleys and major bedrock spillways; therefore the lake levels and extends were very similar throughout the repeated ice advances. During deglaciation the lakes commonly increased in size and eventually drained successively towards the west and northwest into the Lower Rhine Embayment and the North Sea. Catastrophic lake-drainage events occurred when large overspill channels were suddenly opened. Ice-streaming at the end of the older Saalian glaciation was probably triggered by major lake-drainage events.

1. Introduction

During the Middle Pleistocene Saalian glaciation several advances of the Fennoscandian ice sheets reached far into northern central Europe (Fig. 1). Despite the long research history, the correlation between the different stages of ice-sheet advance and decay still remains problematic (cf., Ehlers et al., 2004, 2011; Böse et al., 2012; Lee et al., 2012) and numerical age constraints are sparse. Three major Saalian ice advances with several sub-phases are known from northern Germany (Eissmann, 2002; Litt et al., 2007; Ehlers et al., 2011; Stephan, 2014). These repeated ice advances of the Middle Pleistocene Saalian glaciation are generally correlated with MIS 6 and are referred to as Drenthe and Warthe ice advances (Litt et al., 2007; Ehlers et al., 2011). However, there is increasing evidence of an extensive earlier Saalian ice advance during MIS 8 (Beets et al., 2005; Kars et al., 2012; Roskosch et al., 2015).

Along the Middle Pleistocene Saalian ice-sheets numerous ice-dammed lakes formed in the southern North Sea basin (Gibbard, 2007; Busschers et al., 2008; Cohen et al., 2014, 2017), the Netherlands (Beets and Beets, 2003; Busschers et al., 2008; Laban and van der Meer, 2011), Germany (Eissmann, 1975, 2002; Gassert, 1975; Thome, 1983; Klostermann, 1992; Junge, 1998; Winsemann et al., 2003, 2004, 2007a, b, 2009, 2011a, b, 2016; Meinsen et al., 2011) and Poland (Marks, 2011; Salamon et al., 2013; Marks et al., 2016). However, the size and volume of many

* Corresponding author.
E-mail address: lang@geowi.uni-hannover.de (J. Lang).

https://doi.org/10.1016/j.quascirev.2017.11.029

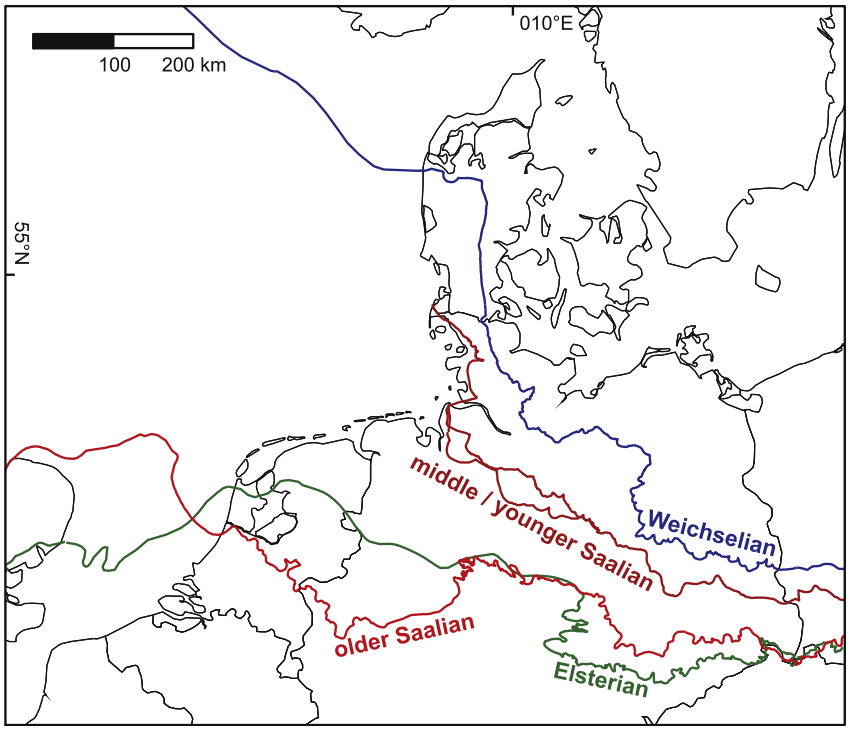

Fig. 1. Overview map, showing the maximum extent of the Middle and Late Pleistocene ice advances. Ice margins are based on Ehlers et al. (2011), Winsemann et al. (2011b) and Moreau et al. (2012).

of these lakes are commonly underestimated because the reconstructions were based on lake-bottom sediments only (Junge, 1998; Eissmann, 2002).

Ice-dammed lakes interact with the dynamics of ice sheets, meltwater and sediments and exert an important control on ice-sheet dynamics by accelerating the ice flow and the loss of ice mass (Stokes and Clark, 2004; Winsborrow et al., 2010; Carrivick and Tweed, 2013; Perkins and Brennand, 2015; Sejrup et al., 2016). Ice streams may be triggered by the effects of proglacial lakes on glacier dynamics (Stokes and Clark, 2003, 2004; Meinsen et al., 2011; Winsemann et al., 2011b). The opening of outlets during ice retreat may cause glacial lake-outburst floods, which have an enormous impact on the subsequent landscape and drainage evolution (Baker, 1973; Gibbard, 2007; Gupta et al., 2007, 2017; Meinsen et al., 2011; Carling, 2013; Collier et al., 2015; Winsemann et al., 2016). The removal of large ice-masses during glacial lake-outburst floods will further destabilise the ice margin, trigger local re-advances and finally contribute to the decay of an ice sheet (Stokes and Clark, 2004; Meinsen et al., 2011; Winsemann et al., 2011b; Sejrup et al., 2016).

The aim of this study is to provide a comprehensive palaeogeographic reconstruction of the spatio-temporal evolution of ice advances, ice-margin configurations and ice-dammed lake systems along the southwestern margin of the Middle Pleistocene Saalian Fennoscandian ice sheets. New and previously published numerical ages are integrated with data on palaeo-ice flow directions and till provenance. The extent and evolution of ice-dammed lakes is based on a detailed facies analysis of ice-marginal deposits, the mapping of fine-grained lake bottom sediments and the mapping of lake-overspill channels.

2. Regional setting

The study area stretches along the former southwestern margin of the Middle Pleistocene Fennoscandian ice sheets (Fig. 1), where the river valleys of the Central German Uplands pass northwards into the low-relief area of the North German Lowlands. The terrain of the Central German Uplands is characterised by up to 400 m high bedrock ridges and relatively steep river valleys. Extensive low relief areas are formed by the Lower Rhine Embayment and the Münsterland Embayment in the west and the Halle-Leipzig lowland area in the east. Most of these bedrock ridges trend WNW to ESE and comprise Mesozoic or Palaeozoic rocks. A distinct west-east division of the study area is caused by the NWN to ESE trending Palaeozoic rocks of the Harz Mountains. The river courses are mainly directed towards the northwest (Fig. 2).

The study area has been affected by multiple ice advances during both the Elsterian and Saalian glaciations. From the Elsterian glaciation two major ice advances are known, which advanced to approximately the same maximum position (Eissmann, 1975, 1994, 1997, 2002; Litt et al., 2007; Ehlers et al., 2011; Roskosch et al., 2015). These ice advances probably occurred during MIS 12 and MIS 10 (Gibbard and Cohen, 2008; Litt et al., 2008; Ehlers et al., 2011; Böse et al., 2012; Lang et al., 2012; Lee et al., 2012; Roskosch et al., 2015). The Saalian Complex in northern central Europe spans MIS 8 to MIS 6 (Fig. 3; Litt et al., 2008). The maximum extent of the Saalian ice cover was reached during the older Saalian glaciation, while the middle and younger Saalian glaciations had lesser maximum extents (Fig. 1; Ehlers et al., 2011). The older Saalian glaciation is commonly referred to as the Drenthe ice advance, while the middle and younger Saalian glaciations are referred to as Warthe ice advances (Litt et al., 2007; Ehlers et al., 2011; Laban and van der Meer, 2011), although the middle Saalian ice advance is locally also referred to as the younger Drenthe ice advance (Hoffmann and Meyer, 1997; Meyer, 2005).

The Saalian glacigenic deposits include subglacial tills, coarse-grained meltwater deposits and fine-grained lake-bottom sediments. Beyond the limits of glacigenic deposition the glaciations

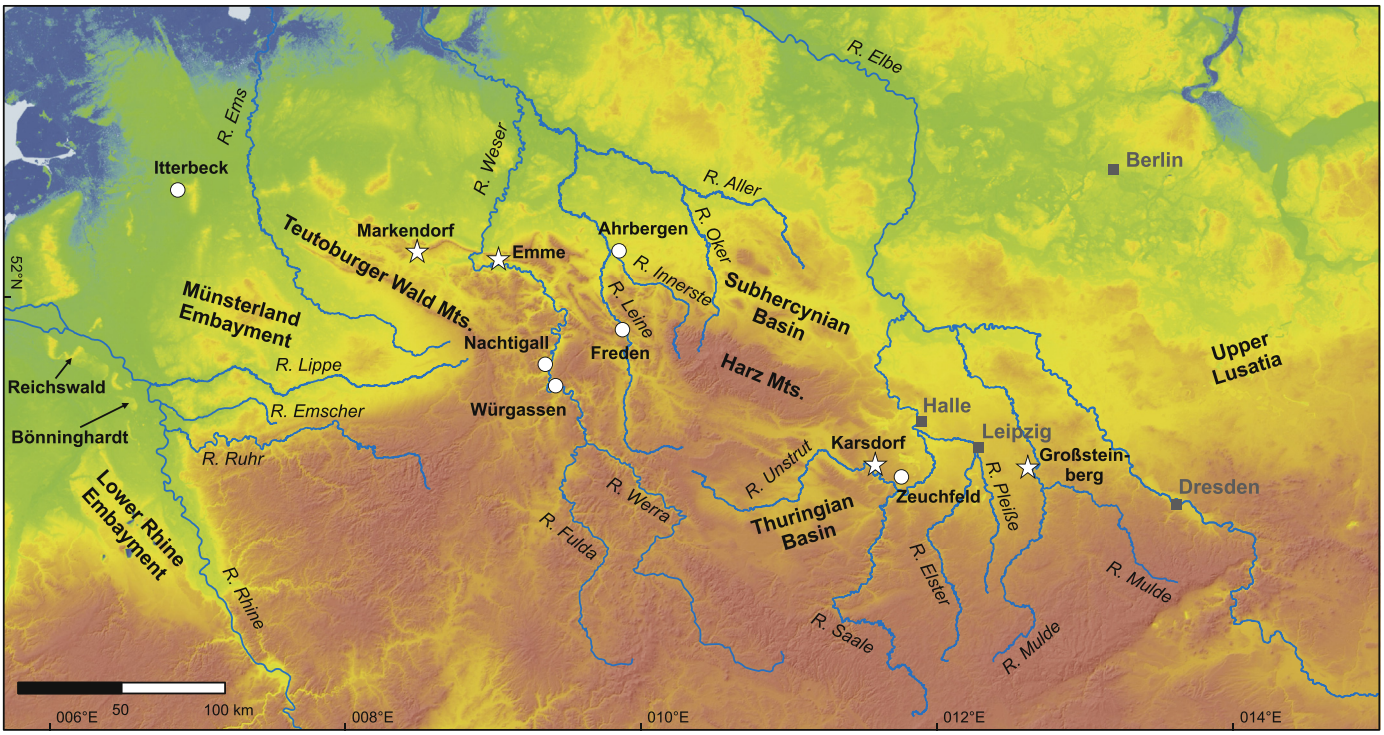

Fig. 2. Overview map of the study area, showing all locations mentioned in the text. White stars indicate the sampling locations for luminescence dating. White circles indicate the locations of numerical ages from previous studies.

were characterised by hill-slope erosion, aeolian and fluvial processes (e.g., Eissmann, 2002; Litt et al., 2007; Winsemann et al., 2015). In lowland areas the regional lithostratigraphic framework is commonly well established due to the vertical stacking of deposits, where tills, lake-bottom sediments and fluvial deposits form laterally extensive lithostratigraphic markers (Caspers et al., 1995; Eissmann, 2002). In upland areas, where the preservation of glacigenic deposits is more patchy and coarse-grained glacilacustrine ice-marginal deposits form rather isolated sediment bodies (Winsemann et al., 2003, 2004, 2007a, b, 2009, 2011a, b), the correlation is more challenging. Numerical dating in combination with a detailed facies analysis has shown that such isolated sediment bodies may include deposits of two different ice advances (Roskosch et al., 2015).

Many previous studies concur with the presence of two to three ice advances during the older Saalian glaciation (Lüttig, 1954, 1960; Eissmann, 1975, 2002; Skupin et al., 1993, 2003). However, the duration and extent of these ice advances is disputed and they have commonly been attributed to ice-front oscillations or changes in ice-flow direction (Meyer, 2005; Litt et al., 2007).

In the western part of the study area three older Saalian ice advances are distinguished by till provenances and ice-advance directions (Skupin et al., 1993, 2003; Skupin and Zandstra, 2010). Only few sites exist in the Münsterland Embayment, where vertically stacked tills of these different older Saalian ice advances have been described (Skupin et al., 1993, 2010; Saloustros and Speetzen, 1999). From the Weser and Leine valleys, Lüttig (1954, 1960) described two older Saalian ice advances, which each deposited a basal till, referred to as the Alfeld and Freden phases. These tills are separated by an erosional unconformity and the lower till (Alfeld phase) displays evidence of weathering and soil formation (Lüttig, 1960).

Probably the most complete record of the Middle Pleistocene ice advances was preserved in the lowland area around Halle and Leipzig, where up to two Elsterian and three older Saalian tills are vertically stacked (Fig. 3; Eissmann, 2002). All these tills are separated by fine-grained glacilacustrine deposits, indicating the repeated formation of proglacial lakes during the advance, maximum extent and retreat of the Elsterian and Saalian ice sheets (Eissmann, 1975, 1994, 2002; Junge, 1998; Junge et al., 1999). The lower Saalian till relates to the more extensive Zeitz phase and the upper two tills to the less extensive Leipzig phase (Fig. 3; Eissmann, 1994, 2002). The local occurrence of fluvial deposits and widespread cryoturbation features in lake-bottom deposits between the tills of the Zeitz and the Leipzig phases (Eissmann, 1975, 2002; Junge et al., 1999) may indicate a longer exposure and the correlation of the Zeitz phase with an early Saalian ice advance.

In spite of the different ice-advance directions and till provenance all ice advances of the Saalian glaciation are correlated with MIS 6 (Lambeck et al., 2006; Busschers et al., 2008; Ehlers et al., 2011; Böse et al., 2012; Lee et al., 2012). This correlation with MIS 6 is commonly based on overlying or underlying non-glacial deposits. Numerical ages determined in modern studies (conducted during the last 15 years) of the Drenthe ice advance are yet sparse (Busschers et al., 2008; Krbetschek et al., 2008; Roskosch et al., 2015; Winsemann et al., 2015, 2016) and range from 196 ± 19 ka to 153 ± 7 ka. The available older age estimates for glacigenic deposits (Krbetschek and Stolz, 1994; Preusser, 1999; Fehrentz and Radke, 2001) range from 150 ± 21 ka to 199 ± 19 ka. However, there is also growing evidence for an earlier Saalian ice advance during MIS 8 or early MIS 6, which occurred between 254 ± 36 and 214 ± 32 ka and reached the southern North Sea, the Netherlands and northwestern Germany (Beets et al., 2005; Meijer and Cleveringa, 2009; Kars et al., 2012; Roskosch et al., 2015).

The subsequent ice advances of the middle and younger Saalian glaciation (Warthe) terminated at the northeastern margin of the study area (Fig. 1; Ehlers, 1990; Meyer, 2005; Ehlers et al., 2011). Luminescence dating of deposits of the Warthe ice advance from

Lithostratigraphic units in northern and central Germany (Lüttig, 1954; Eissmann, 2002; Skupin et al., 2003; Litt et al., 2007; Ehlers et al., 2011)				Ice-dammed lakes	Numerical ages (**bold:** this study)
		Western study area	Eastern study area		
Middle Pleistocene Saalian Complex (MIS 8 to MIS 6)	Younger Saalian glaciation	Warthe II	Warthe / Fläming		Glacifluvial deposits (NE Germany): 155 ± 21 ka, 150 ±14 ka, 138 ± 10 ka, 131 ± 10 ka and 130 ± 17 ka (Lüthgens et al., 2010); 139 ± 17 ka (Kenzler et al., 2017)
	Middle Saalian glaciation	Warthe I (also "Drenthe II")			
	Older Saalian glaciation	Drenthe (also "Drenthe I", "Main Drenthe" or "Hameln phase") – Freden phase	Leipzig phase – Rabutz clay	lake drainage	**Glacifluvial delta deposits (Weser Lake): 171 ± 21 ka (Fe-1-16),156 ± 24 ka (Fe-2-16) and 157 ± 16 ka (Ma-1-16)**
			Second Saalian till (upper unit)		Outburst-flood deposits (Weser Lake): 153 ± 7 ka and 139 ± 8 ka (Winsemann et al., 2016)
			Breitenfeld clay	lake formation	Glacifluvial delta deposits (Leine Lake): 196 ± 19 ka and 161 ± 10 (Roskosch et al., 2015)
			Second Saalian till (lower unit)	lake drainage (?)	**Glacifluvial delta deposits (Halle-Leipzig Lake): 175 ± 10 ka (Kar-U)**
			Bruckdorf clay (advance)	lake formation	**Glacifluvial delta deposits (Halle-Leipzig Lake): 173 ± 19 ka (GS-1-17)**
				cryoturbation, fluvial erosion and deposition, soil formation	
		Alfeld phase	Zeitz phase – Bruckdorf clay (retreat)	lake drainage	Glacifluvial deposits (NW Germany): 248 ± 22 ka (Kars et al., 2012)
			First Saalian till		Glacifluvial delta deposits (Leine Lake): 250 ± 20 and 241 ± 27 ka (Roskosch et al., 2015)
			Böhlen-Lochau clay	lake formation	Glacifluvial delta deposits (Saale-Unstrut Lake): 323 ± 70 ka (Kreutzer et al., 2014)
	Early Saalian	Middle terrace	Main terrace complex		Fluvial deposits (central Germany): 306 ± 23 ka, 277 ± 22 ka, 268 ± 20 ka, 272 ± 23 ka and 227 ± 15 ka (Krbetschek et al., 2008)

Fig. 3. Stratigraphic chart for the Middle Pleistocene Saalian complex in northern central Europe, summarising lithostratigraphic units, ice-dammed lake evolution and numerical ages.

northeastern Germany yielded ages between 155 and 130 ka (Lüthgens et al., 2010; Kenzler et al., 2017).

3. Database and methodology

The palaeogeographic reconstruction of ice advances and proglacial lakes draws on the evaluation of an extensive database of previous regional lithostratigraphic studies, geological maps (1:25,000, 1:50,000, 1:100,000), borehole logs and outcrops. The relevant information includes mapped ice-marginal deposits, the distribution of glacigenic deposits, data on ice-advance directions and till provenance. The available geological information was integrated in a geographical information system (Esri ArcGIS, Version 10.3). Optically-stimulated luminescence ($pIRIR_{290}$) dating of feldspar grains was applied to get numerical ages for the studied deposits at selected locations.

3.1. Reconstruction of ice advances

The different ice advances into the study area were reconstructed based on ice-marginal deposits, indicators of the ice-advance direction and till provenance.

3.1.1. Palaeo-ice marginal positions

Palaeo-ice marginal positions have been mapped across the study area and include bodies of meltwater deposits, as sandurs, glacifluvial deltas and subaqueous ice-contact fans and push and dump moraines. Most mapped ice-marginal positions relate to the maximum ice-sheet extent or stillstand positions during ice-margin retreat (Eissmann, 1975, 1997, 2002; Van der Wateren, 1987; Feldmann, 1997; Reinecke, 2006; Winsemann et al., 2007a, b, 2009; 2011b; Meng and Wansa, 2008; Skupin and Zandstra, 2010). Prominent morainal ridges may exceed the surrounding lowlands by 10–80 m. Some morainal ridges display a high lateral continuity and can be traced for more than 50 km, while others form laterally discontinuous isolated ridges. The connection of separated morainal ridges to reconstruct the palaeo-ice margins has been a matter of debate (cf., Eissmann, 1997, 2002; Böse et al., 2012). However, the mapped morainal ridges provide a relatively coherent picture of the palaeo-ice margins during the more pronounced phases of stillstands during overall ice-margin retreat.

3.1.2. Ice-flow indicators and till provenance

An extensive database of regional studies provides data on the palaeo-ice flow direction and till provenance. Reconstructions of the ice-flow direction are based on clast alignment within tills, glacitectonic deformation structures at various scales, glacial striations and mega-scale glacial lineation. Mega-scale glacial lineations were mapped from digital elevation models (grid ~30 m, vertical accuracy ~3 m (EU-DEM) and grid ~10 m, vertical accuracy ± 0.5 m (Bezirksregierung Köln)) of the western part of the study area. In some areas, several generations of mega-scale glacial lineations could be identified based on cross-cutting relationship, following the criteria established by Clark (1993) and Boulton et al. (2001). Comprehensive maps of palaeo-ice flow directions for parts of the study area have previously been published by Eissmann

(1975), Ehlers and Stephan (1983, 1990), van den Berg and Beets (1987), Zandstra (1987), Höfle (1991), Skupin et al. (1993) and Skupin and Zandstra (2010).

The provenance of clasts within tills and other glacigenic deposits has long been used to distinguish between deposits of the different ice advances. These studies rely on the identification of indicator pebbles from source areas in Fennoscandia or the Baltic region. For the western part of the study area comprehensive maps of the clast provenance are provided by Zandstra (1987), Skupin et al. (1993), Speetzen and Zandstra (2009) and Skupin and Zandstra (2010). For the eastern part of the study area such comprehensive maps are lacking; however, a number of studies, containing clast-provenance data, exist (e.g., Eissmann, 1975, 1994, 1997; Hoffmann and Meyer, 1997). Additional clast-provenance data from across the study area from Lüttig (1954, 1958) and Winter (1998) were included in the database.

3.2. Reconstruction of ice-dammed lakes

The reconstruction of ice-dammed lakes is based on the mapping of glacilacustrine deposits, lake-overspill channels and the identification of potential damming locations (cf., LaRocque et al., 2003; Stokes and Clark, 2004; Winsemann et al., 2009, 2011a, b; Perkins and Brennand, 2015; Brouard et al., 2016; Gorlach et al., 2017). In outcrop, sedimentary sections were logged in detail and the large-scale facies architecture was mapped from photo panels. Glacilacustrine deposits in the study area include ice-contact deltas and subaqueous ice-contact fans, fluvial and glacifluvial deltas (Table 1) and fine-grained lake-bottom deposits (Table 2).

Ice-contact deltas are deposited by meltwater streams discharging directly from the ice-margin into the lake, while glacifluvial deltas are characterised by a delta plain, separating the ice margin and the lake (Hambrey, 1995; Lønne, 1995). If preserved, the foreset-topset transition represents a reliable indicator for the palaeo-lake level and the reconstruction of ice-dammed lakes (Winsemann et al., 2011a; Perkins and Brennand, 2015). Fluvial deltas may form in high-relief settings, where tributary rivers enter the valley of their trunk river.

Subaqueous ice-contact fans are deposited by sediment-laden meltwater discharging from subglacial conduits. Providing sufficient sediment supply and time, a subaqueous fan may aggrade to the lake surface and evolve into a delta (Powell, 1990; Lønne, 1995; Winsemann et al., 2009). Fine-grained glacilacustrine or lake-bottom deposits are widespread in the study area and comprise massive clay, planar-parallel laminated and ripple cross-laminated silt and fine-grained sand (Junge, 1998; Junge et al., 1999; Winsemann et al., 2009, 2011b). Fine-grained glacilacustrine deposits are mainly derived from suspension fall-out and waning low-density turbidity currents in ice-distal settings (Hambrey, 1995). Deposits of subaqueous ice-contact fans and fine-grained lake-bottom deposits will provide an underestimation of the palaeo-water plane (Winsemann et al., 2009, 2011b; Perkins and Brennand, 2015).

Potential damming locations and lake overspills are identified from the digital elevation model. Lake spillways are commonly characterised by deep v-shaped gorges incised into bedrock ridges (Thome, 1983; Kehew and Lord, 1986; LaRocque et al., 2003; Meinsen et al., 2011; Perkins and Brennand, 2015; Winsemann et al., 2016). In front of the overspills features as trench-like channels, isolated scours, streamlined hills and thick fan-shaped accumulations of meltwater deposits are indicative of high discharges during lake-outburst floods (Baker, 1973; Carling et al., 2009a, b; Meinsen et al., 2011; Winsemann et al., 2016). The elevation of lake spillways represents an underestimation of the lake level due incision during overspill or lake-outburst floods (LaRocque et al., 2003; Perkins and Brennand, 2015).

Table 1
Overview of the coarse-grained glacilacustrine sediment bodies identified in the study area.

Lake system	Name	Number on map	Ice advance	Interpretation	Elevation (m a.s.l.)		Reference for description
					Base	Top	
Weser Lake							
	Markendorf	1	2nd	Glacifluvial delta	100	125	Skupin et al., 2003
	Porta	2	1st	Subaqueous ice-contact fan/Glacifluvial delta	70	130	Hornung et al., 2007; Winsemann et al., 2007a, 2011b
	Emme	3	2nd	Glacifluvial delta	95	165	Winsemann et al., 2004, 2011a
	Coppenbrügge	4	1st	Subaqueous fan/Delta	90	170	Winsemann et al., 2003, 2004, 2007a, 2011b
Leine Lake							
	Freden	5	1st and 2nd	Glacifluvial delta	110	185	Winsemann et al., 2007b, 2011b; Roskosch et al., 2015
	Bornhausen	6	1st	Glacifluvial delta	160	190	Winsemann et al., 2007b, 2011b
	Wallmoden	7	1st	Glacifluvial delta	165	180	Feldmann and Meyer, 1998
Subhercynian Lake							
	Wasserleben	8	?	Glacifluvial delta	?	176	Reinecke, 2006
	Zilly	9	?	Glacifluvial delta	?	180	Reinecke, 2006
	Warnstedt	10	?	Glacifluvial delta	?	192	Reinecke, 2006
	Badeborn	11	?	Glacifluvial delta	160	175	Reinecke, 2006
	Ströbeck	12	?	Subaqueous ice-contact fan (mid-fan to distal fan deposits)	150	180	Reinecke, 2006
	Derenburg	13	?	Subaqueous ice-contact fan (mid-fan to distal fan deposits)	?	165	Reinecke, 2006
Saale-Unstrut Lake							
	Zeuchfeld	14	1st	Glacifluvial delta	105	195	Ruske, 1961; Eissmann, 2002; Meng and Wansa, 2008
	Karsdorf	15	2nd	Glacifluvial delta	125	140	Meng and Wansa, 2008
	Schmon	16	?	Glacifluvial delta	173	188	Gassert, 1975; Schuberth and Radzinski, 2014
Halle-Leipzig Lake							
	Niederwünsch	17	?	Glacifluvial delta	130	150	Meng and Wansa, 2008
	Großsteinberg	18	2nd	Glacifluvial delta	130	155	–
	Sachsendorf	19	2nd	Glacifluvial delta	135	170	–
Mulde Lake							
	Großbothen	20	1st	Glacifluvial delta	150	175	Eissmann and Müller, 1994

Table 2
Overview of fine-grained lake-bottom deposits described in the study area.

Lake system	Stage of ice advance	Elevation (m a.s.l.)	Thickness (m)	Reference
Northwestern Germany				
Weser Lake	Maximum/retreat	55–180	0.5–20	Junge, 1998; Winsemann et al., 2009, 2011b
Leine Lake	Maximum/retreat	80–190	0.1–20	Winsemann et al., 2007b, 2011b
Harz Mountains and Subhercynain Basin				
Harz Lakes (several small river valleys)	Maximum	130–320	1–8	Pilger et al., 1991; Reinecke, 2006
Central and eastern Germany				
Saale-Unstrut Lake	Maximum/retreat	123–200	0.2–9.5	Ruske and Wünsche, 1964; Junge, 1998
Pleiße Lake	Maximum	125–175	0.1–0.5	Junge, 1998
Mulde Lake	Maximum	148–190	0.1–3 (max. 15)	Junge, 1998
Elbe Lake	Maximum	110–222	0.4–5	Wolf et al., 1994; Junge, 1998; Eissmann, 2002; Huhle, 2015
Elbe Lake	Retreat	100–170	0.5–3	Grahmann and Kossmat, 1927; Grahmann, 1929; Härtel, 1941
Halle-Leipzig Lake ("Böhlen-Lochau clay")	Advance/ maximum	95–150	0.2–0.7	Eissmann, 1975, 1997, 2002; Junge, 1998
Halle-Leipzig Lake ("Bruckdorf clay")	Retreat	79–155	0.5–5	Grahmann, 1925; Bettenstaedt, 1934; Schulz, 1962; Mahenke and Grosse, 1970; Eissmann, 1975; Junge, 1998; Junge et al., 1999
Halle-Leipzig Lake ("Bruckdorf clay")	Advance/ maximum	100–120	0.5–11	Eissmann, 1975, 1997, 2002; Junge, 1998; Junge et al., 1999
Halle-Leipzig Lake ("Breitenfeld clay")	Advance/ maximum	120–135	0.2–3	Eissmann, 1975

3.2.1. Reconstruction of the lake areas and volumes

A geographical information system was used to compile all identified glacilacustrine deposits, overspills and possible drainage pathways. Extends and volumes of the ice-dammed lakes were reconstructed in ArcGIS and are based on a digital elevation model (resolution ~30 m, vertical accuracy ~3 m; EU-DEM). After the identification of the lake-level and the dam location, the ice-margin responsible for the damming and contour line corresponding to the elevation of the lake level were intersected and extracted to obtain the outline and the area of the lake. The lake volume was calculated using the ArcGIS 3D analyst toolbox, which allows calculating the volume enveloped by the digital elevation model and an intersecting horizontal plane. Similar workflows have previously been applied by LaRocque et al. (2003), Stokes and Clark (2004), Winsemann et al. (2007a, b, 2009, 2011b, 2016), Perkins and Brennand (2015), Brouard et al. (2016) and Gorlach et al. (2017).

3.3. Optically-stimulated luminescence dating

3.3.1. Sampling and sample preparation

Samples for optically-stimulated luminescence dating (OSL) were collected from different locations (Fig. 2), using light tight steel tubes. Unfortunately, many pits have been refilled and sampling was no longer possible. Samples for gamma spectrometry were taken at equal position as the samples for OSL dating. Sample preparation and measurement for OSL dating was applied in the luminescence-dating laboratory of the Department of Human Evolution, Max Planck Institute for Evolutionary Anthropology, Leipzig. Sample preparation was conducted under subdued red light. The dried material was first sieved to obtain the preferred grain-size fraction (180–250 μm). The chemical treatment included a removal of carbonates by digestion in HCl, and of organic matter by digestion in H_2O_2. To extract K-feldspar among minerals, density separation was used to remove heavy minerals and quartz using lithium heterotungstate.

Finally, the sample material was mounted on steel discs (aliquots) using silicon spray. Equivalent dose (De) measurements were undertaken using automated Risø TL-DA-20 reader equipped with IR light-emitting diodes transmitting at 870 nm (145 mW/cm^2). Irradiation was provided by a calibrated $^{90}Sr/^{90}Y$ beta source with a dose-rate of ~0.24 Gy/s. The signal was detected through a D-410 filter (Chroma Technology Corp., Bellows Falls, USA), allowing detection in the blue-violet wavelength range.

3.3.2. Dose rate

Dose rates were determined based on high-resolution germanium gamma spectrometric analysis of the radioactivities of uranium, thorium, potassium and their daughter isotopes, undertaken on the bulk sediment samples at the "Felsenkeller" laboratory (VKTA) in Dresden (Tables 3 and 4). Dose rate attenuation by moisture was accounted for using water content values of 10 ± 10%. Such a high uncertainty was chosen to account for the potential variation of water content during the length of burial. The cosmic ray component of the dose rate was calculated based on Prescott and Hutton (1994). The internal potassium content was assumed to be at 12.5 ± 0.5% (Huntley and Baril, 1997). Dose-rate conversion factors were taken from Guérin and Mercier (2011). To account for alpha efficiency an a-value of 0.11 ± 0.02 was used (e.g., Kreutzer et al., 2014b). Table 3 gives an overview on the obtained nuclide concentrations and the total dose rates.

3.3.3. Equivalent dose estimation

K-feldspar was chosen for luminescence dating of the investigated sites as it saturates at much higher doses than quartz (e.g., Roskosch et al., 2015) and therefore provides the possibility to date back several 100 ka. Nevertheless, the feldspar luminescence signal measured at lower temperatures (e.g., 50 °C) is mostly affected by anomalous fading (Wintle, 1973), causing age underestimation if not accounting for it.

Fading corrections for feldspar grains, yielding luminescence signals plotting beyond the linear part of the dose-response curve, are problematic (Huntley and Lamothe, 2001; Kars et al., 2008). Therefore, methodological research on feldspar-luminescence dating within the last decade concentrated on stimulating luminescence from electron traps, which are not or only to a negligible part affected by fading (e.g., Buylaert et al., 2009; Thiel et al., 2011; Lauer et al., 2012; Frouin et al., 2017).

It was demonstrated that reliable feldspar luminescence ages can be obtained by stimulating the feldspar signal at elevated temperatures after depleting the IR_{50}-signal (Thomsen et al., 2008). For those so called pIRIR signal fading rates are very low or even non-detectable. Especially for the $pIRIR_{290}$ dating approach, very

Table 3
Nuclide concentrations, cosmic dose rate and calculated total dose rate (DR_{total}).

Sample Code	Lab.- ID	U (ppm)	Th (ppm)	K (%)	Cosmic Dose (Gy/ka)	DR_{total} (Gy/ka)
Ma-1-16	1542	0.80 ± 0.15	2.19 ± 0.16	1.16 ± 0.10	0.10 ± 0.01	1.99 ± 0.16
Fe-1-16	1546	1.18 ± 0.20	3.81 ± 0.26	0.90 ± 0.08	0.17 ± 0.02	2.01 ± 0.21
Fe-2-16	1547	1.33 ± 0.22	4.18 ± 0.29	1.00 ± 0.09	0.17 ± 0.02	2.16 ± 0.21
Kar-U	1550	1.61 ± 0.28	6.16 ± 0.40	2.57 ± 0.21	0.12 ± 0.01	3.71 ± 0.21
GS-1-17	1606	0.77 ± 0.21	2.55 ± 0.18	1.49 ± 0.11	0.17 ± 0.02	2.37 ± 0.22

Table 4
Summary of the luminescence dating results. The equivalent dose values (De) are based on the $pIRIR_{290}$ dating approach and were calculated using the central age model (CAM) as well as the median. For sample Fe-2-16, additionally the minimum age model (MAM3; Galbraith et al., 1999) was used because of the high overdispersion of De-values. The MAM3 De-value is at 335.5 ± 41 Gy. Dose rates (DR) were obtained using high resolution gamma spectrometry (OD: Overdispersion; Nr. al: Number of aliquots fulfilling the acceptance criteria; DR ratio: measured-to-given dose ratio from dose-recovery test).

Sample Code	Lab.- ID	De (Gy); CAM	De (Gy); median	Age (ka); CAM	Age (ka); Median	Age (ka); MAM3	OD %	Nr. al	G-value ($pIRIR_{290}$)	DR ratio
Ma-1-16	1542	332 ± 18	312 ± 20	167 ± 16	157 ± 16	–	26	20	1.5 ± 0.4	1.08 ± 0.05
Fe-1-16	1546	373 ± 26	344 ± 21	185 ± 23	171 ± 21	–	25	16	–	–
Fe-2-16	1547	449 ± 32	435 ± 36	208 ± 25	201 ± 26	156 ± 24	30	24	–	–
Kar-U	1550	657 ± 10	650 ± 10	177 ± 10	175 ± 10	–	8	23	–	1.17 ± 0.06
GS-1-17	1606	418 ± 23	409 ± 23	176 ± 19	173 ± 19	–	24	20	–	–

high signal stability can be assumed and fading corrections are probably not necessary.

Nevertheless, it was also highlighted that feldspar signals measured at elevated temperatures are characterised by a hard to bleach luminescence component (e.g., Kars et al., 2012; Buylaert et al., 2012; Colarossi et al., 2015), which might cause age overestimation if partly insufficient bleached deposits are dated. Li and Li (2011) demonstrated that the bleachability decreases with increasing stimulation temperature.

In this study we applied the $pIRIR_{290}$ approach following the measurement-procedure as outlined by Thiel et al. (2011). The K-feldspar IRSL signal is first measured at 50 °C followed by the detection of the pIRIR-signal at 290 °C (Table 4; Fig. 4). For age calculation the 290 °C signals were used, which are characterised by high signal-stability and fading corrections are thus not mandatory anymore (Buylaert et al., 2012). To create a dose response-curve four regenerative dose points were given after measuring the natural IRSL-signal (Lx/Tx). At the end of each pIRIR SAR-cycle, the recycling ratio was determined, hence, the first dose point was re-measured and subsequently all aliquots showing recycling ratios deviating >10% from unity were rejected. Furthermore, only aliquots for which a recuperation of <5% was observed were used for De-calculation.

To address the effect of insufficient bleaching we measured very small aliquots (1 mm average), hosting only a few K-feldspar grains per disc. Hence, scatter among the equivalent dose distribution can be outlined and outliers in the upper De-range can be excluded from age-calculations.

Nevertheless, we are aware of the fact that the here presented luminescence-age estimates have to be discussed in terms of potential age overestimation. Dose residuals surely effect the age calculation but for Middle Pleistocene samples hosting mean-equivalent doses above 300 Gy, the percentage of residuals among the total equivalent dose might be rather small.

3.3.4. Dose recovery tests

The applied $pIRIR_{290}$-protocol was tested on its resilience by applying dose-recovery tests on samples Ma-1-16 and Kar-U.

Six aliquots were bleached for 2 h under a solar-lamp. In a next step, equivalent dose residuals were measured. The remaining three aliquots were beta-irradiated with a well-known dose which

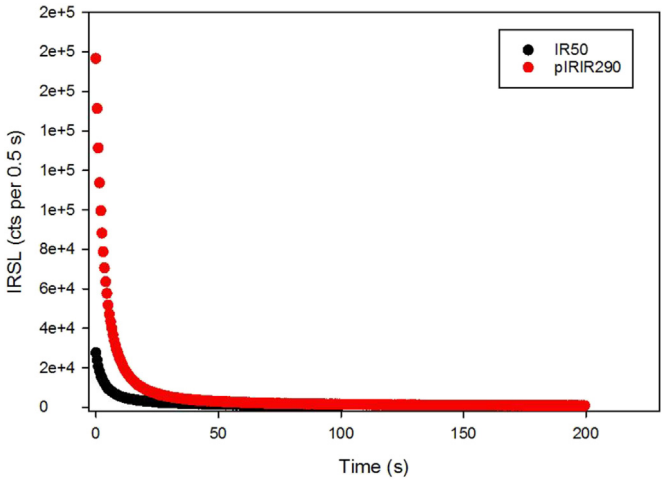

Fig. 4. Decay curves (IR_{50} and $pIRIR_{290}$) obtained from sample Ma-1-16.

was selected be close to the natural dose and it was tested on how precise the $pIRIR_{290}$-protocol can recover the inserted dose.

The residual-subtracted measured-to-given dose ratios are at 1.08 ± 0.05 for sample Ma-1-16 and at 1.17 ± 0.06 for sample Kar-U (Table 4). Hence, the dose-recovery result obtained from sample Ma-1-16 is deviating <10% from unity whereas the given dose from sample Kar-U is more clearly overestimated. That potential methodological uncertainty has to be kept in mind when discussing the here presented $pIRIR_{290}$ luminescence dating results. The obtained dose-residuals illustrate the lower bleachabilty of the $pIRIR_{290}$-signal compared to the IR_{50}-signal. The $pIRIR_{290}$ residuals measured after 2 h of solar-lamp exposure are at 37.5 ± 2.7 Gy (sample Ma-1-16) and 40.8 ± 2.0 Gy (sample Kar-U), whereas the IR_{50} residuals are only at 9.4 ± 0.5 Gy and 11.3 ± 0.5 Gy, respectively.

3.3.5. Fading

Even if $pIRIR_{290}$ feldspar signals are not or only to a negligible part effected by anomalous fading (Buylaert et al., 2012), it is recommended to quantify the potential signal loss for the pIRIR-signals. For sample Ma-1-16 fading measurements based on

Huntley and Lamothe (2001) were conducted. Fading was measured on six aliquots. The $pIRIR_{290}$ mean g-value is at 1.5 ± 0.4 (Ma-1-16), illustrating the high signal stability of the $pIRIR_{290}$ signal. The IR_{50} g-value shows a significantly higher signal-loss and is at 4.0 ± 0.8.

3.3.6. Equivalent dose distribution and luminescence-age estimates

The obtained De-distributions show that insufficient bleaching should be taken into account (Fig. 5). However, the De-overdispersions of mostly <30% illustrates that dose residuals should have no significant impact on final De-values, except for sample Fe-2-16 yielding an overdispersion of 30%. To exclude significant outliers within the De-data set, the Central Age Model (CAM; Galbraith et al., 1999) was applied. Additionally, the median De-value was calculated for each sample. Only for sample Fe-2-16 the Minimum Age Model (MAM3; Galbraith et al., 1999) was used for De-determination (Fig. 5).

4. Results

The integration of the available data on ice-advance directions, till provenance, ice-marginal positions, depositional systems and numerical ages allows for the reconstruction of three main ice advances during the older Saalian glaciation. Ice-dammed lake formation occurred during all ice advances and was in each case controlled by the changing ice-margin configuration during ice-sheet advance, maximum and decay. An overview of the lake levels, extents and volumes of the different reconstructed ice-dammed lakes is provided in Table 5.

4.1. First older Saalian ice advance

4.1.1. Ice-flow directions and till provenance

The first Saalian ice advance into the study area in most locations corresponds to the maximum extent of the Saalian glaciation. The ice sheet extended into the eastern Netherlands, the Lower Rhine and Münsterland Embayments, the valleys of Rivers Weser and Leine, the northern margin of the Harz Mountains, the Halle-Leipzig Lowland area and the valley of River Elbe (Fig. 6A). The main ice-flow direction was from north to south. Radial spreading of the ice flow occurred as the ice sheet entered the lowland areas of the Lower Rhine, Münsterland and Halle-Leipzig Embayments (Eissmann, 1975, 2002; Zandstra, 1987; Ehlers, 1990; Skupin et al., 1993, 2003; Ehlers et al., 2011). Mega-scale glacial lineations related to the first ice advance in northwestern Germany trend north-northwest to south-southeast (Fig. 7). In the western part of the study area, till-provenance analyses indicate a dominance of clasts from southern Sweden (>50%; Zandstra, 1987; Skupin et al., 1993, 2003, 2010; Speetzen and Zandstra, 2009). In the eastern part of the study area, till-provenance analyses point to an origin from southern and central Sweden (Hoffmann and Meyer, 1997). This first Saalian ice advance corresponds to the Zeitz phase in eastern Germany (Eissmann, 1975, 2002; Litt et al., 2007; Ehlers et al., 2011) and the first ice advance of the Drenthe advance (Alfeld phase) in western Germany (Lüttig, 1954; Skupin et al., 2003). Unfortunately, many pits exposing sediments of the first ice advance have already been refilled.

4.1.2. Numerical ages

Numerical ages from locations, which can be attributed to the

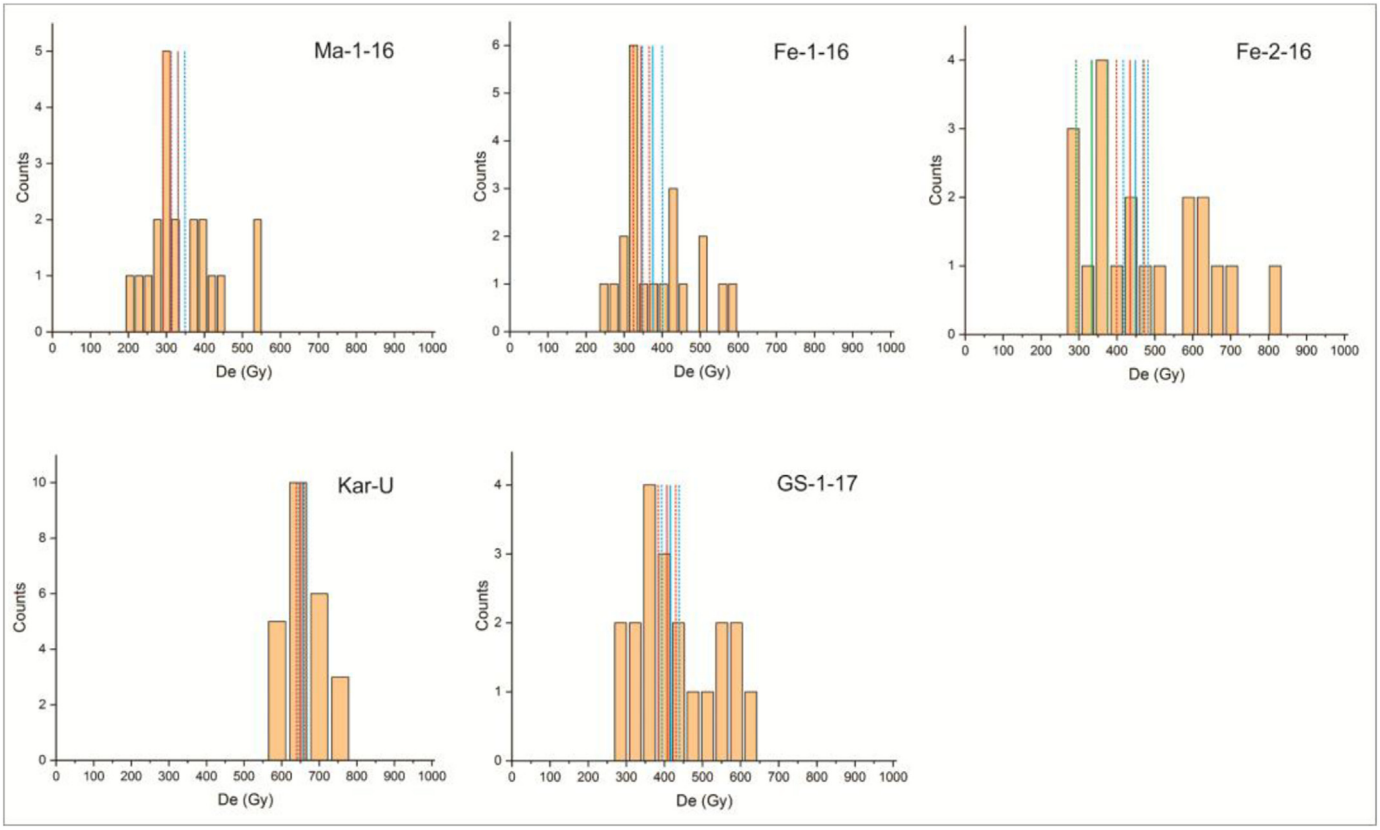

Fig. 5. De-distributions of the measured samples (blue lines: Central Age Model; red lines: Median value; green lines: Minimum Age Model). (For interpretation of the references to colour in this figure legend, the reader is referred to the web version of this article.)

Table 5
Physical characteristics of the ice-dammed lakes, reconstructed for the different ice advances and ice-margin configurations.

Lake System	Ice advance	Stage of ice advance	Lake-level elevation (m a.s.l.)	Area (km^2)	Volume (km^3)	Figure
Northwestern Germany						
Münsterland Lake [a]	1st	Maximum	350	502	45	8A
Münsterland Lake	1st	Retreat	105	2580	75	8B
Münsterland Lake (south)	2nd	Maximum	70	310	2	9A
Münsterland Lake (east)	2nd	Maximum	170	312	11	9A
Münsterland Lake	2nd	Retreat	75	1998	26	9B
Weser Lake [b]	1st and 2nd	Maximum	200	1870	120	8A, 9A
Weser Lake	1st and 2nd	Retreat	135	1123	42	8B, 9B
Weser Lake	1st and 2nd	Retreat	80	293	5	8C
Leine Lake [b]	1st and 2nd	Maximum	200	900	36	8A, 9A
Leine Lake	1st and 2nd	Retreat	135	310	12	8B, 9B
Harz Mountains and Subhercynian Basin						
Harz Lakes	?	Maximum	300	25	1	8A, 9A
Subhercynian Lake	?	Retreat	190	340	8	8B, 9B
Central and eastern Germany						
Saale-Unstrut Lake	1st	Maximum	190	1777	61	8A
Elster, Pleiße and Mulde Lakes	1st	Maximum	190	229	4	8A
Halle-Leipzig Lake [c]	1st	Retreat	190	3326	117	8B
Halle-Leipzig Lake [c]	1st	Retreat	160	6245	224	8C
Halle-Leipzig Lake[c]	2nd	Maximum	160	2235	50	9A

[a] Winsemann et al., 2016.
[b] Winsemann et al., 2011b.
[c] Including the valleys of the Rivers Unstrut, Saale, Elster, Pleiße and Mulde.

first older Saalian ice advance are so far sparse. Kars et al. (2012) estimated quartz ages of 254 ± 32 and 214 ± 36 ka and feldspar ages of 252 ± 21 and 248 ± 22 ka in samples from meltwater deposits from Itterbeck in northwestern Germany. However, Kars et al. (2012) applied a fading correction and did not evaluate potential insufficient bleaching and therefore, an age-overestimation cannot be excluded. The age of meltwater deposits from the northern margin of the Münsterland Embayment, which are overlain by a till of the first older Saalian ice advance (Skupin et al., 1993), ranges from 100 to 250 ka (Fehrentz and Radtke, 2001). Deposits of the lower Freden delta in the Leine valley were dated by Roskosch et al. (2015), resulting in pIR-IR ages of 241 ± 27 and 250 ± 20 ka.

In the Unstrut valley glacifluvial delta deposits at Zeuchfeld yielded a quartz minimum age (in saturation) of 179 ± 51 ka and an IR-RF feldspar age of 323 ± 70 ka (Kreutzer et al., 2014a) and thus indicate that the sedimentary succession at Zeuchfeld was deposited prior to MIS 6. The quartz age only yields a minimum age and the IR-RF age might be overestimated due to insufficient bleaching. Nevertheless, an age overestimation of around 200 ka due to IR-RF dose residuals is unlikely. An earlier deposition during the Elsterian glaciation is unlikely, based on the regional lithostratigraphic correlation (Ruske, 1961; Eissmann, 1975).

Fluvial sediments from several locations in eastern Germany, which were deposited prior to the Saalian glaciation, were dated using infrared radiofluorescence, yielding ages ranging from 306 ± 23 to 227 ± 15 ka (Krbetschek et al., 2008).

4.1.3. Formation of ice-dammed lakes during maximum ice extent

4.1.3.1. Western part of the study area (Münsterland Embayment, Weser and Leine valleys, Harz Mountains). The Münsterland, Weser and Leine Lakes attained their largest extends and volumes during or close to the maximum ice advance (Fig. 8A). The Münsterland Lake had a lake level of 350 m a.s.l., an extent of ~502 km^2 and a volume of ~45 km^3 (Herget, 1998; Meinsen et al., 2011; Winsemann et al., 2016). Major overspill channels were located along the southern margin of the Münsterland Lake at elevations ranging from 350 to 80 m a.s.l. (Thome, 1983; Herget, 1998; Winsemann et al., 2016). Overspills, controlling the lake level of the Weser Lake, have elevations of 205 to 80 m a.s.l. The lake level of the Leine Lake was controlled by overspill elevations of 197 to 115 m a.s.l. Lake-level highstands of the Weser and Leine Lakes of up to 200 m a.s.l. are indicated by overspill channels, deltas and lake-bottom sediments (Tables 1 and 2; Winsemann et al., 2003, 2004, 2007b, 2011a, b; Roskosch et al., 2015). During the lake-level highstand of approximately 200 m a.s.l. the Weser Lake covered an area of 1870 km^2 and had a volume of 120 km^3, while the Leine Lake covered an area of 900 km^2 and had a volume of 36 km^3 (Winsemann et al., 2011b, 2016). A connection between the Weser Lake and the Leine Lake was established via a west-east trending valley, if the lake levels exceeded 197 m a.s.l. (Winsemann et al., 2007b, 2011b). At the eastern lake margin the Leine Lake received overspilling flows from lakes dammed at higher elevations in front of the Harz Mountains, which contributed to the accumulation of the Bornhausen delta (Winsemann et al., 2007b, 2011b).

At the northern margin of the Harz Mountains small, partly interconnected lakes formed in the steep river valleys during the maximum extent of the ice advance (Fig. 8A; Pilger et al., 1991; Junge, 1998; Eissmann, 2002). Fine-grained glacilacustrine deposits occur at elevations between 220 and 330 m a.s.l. (Pilger et al., 1991; Junge, 1998; Reinecke, 2006), providing a minimum elevation for the lake levels. The ice margin reached elevations of 300–360 m a.s.l. (Pilger et al., 1991), indicating the maximum lake-level elevation before overspilling. The water volumes stored in these lakes were rather small, summing up to ~1 km^3.

4.1.3.2. Eastern part of the study area (Thuringian Basin, Halle-Leipzig area and Elbe valley). In the eastern part of the study area extensive ice-dammed lakes formed during the ice-sheet advance and attained lake-level highstands when the ice sheet reached its maximum extent (Fig. 8A; Eissmann, 1975, 1997, 2002). All northwards directed drainage in this area was blocked when the ice margin reached a WNW-ESE trending ridge of Palaeozoic bedrock, which has an elevation of 140–230 m a.s.l. Fine-grained lake-bottom deposits, locally known as Böhlen-Lochau clay, commonly underlie the basal till of the first Saalian ice advance (Zeitz phase) or occur within the valleys of the Rivers Unstrut, Saale, Elster, Pleiße, Mulde and Elbe (Table 2; Junge, 1998; Eissmann, 2002). Thick accumulations of meltwater deposits in the valleys of the River Unstrut and Mulde, which have previously

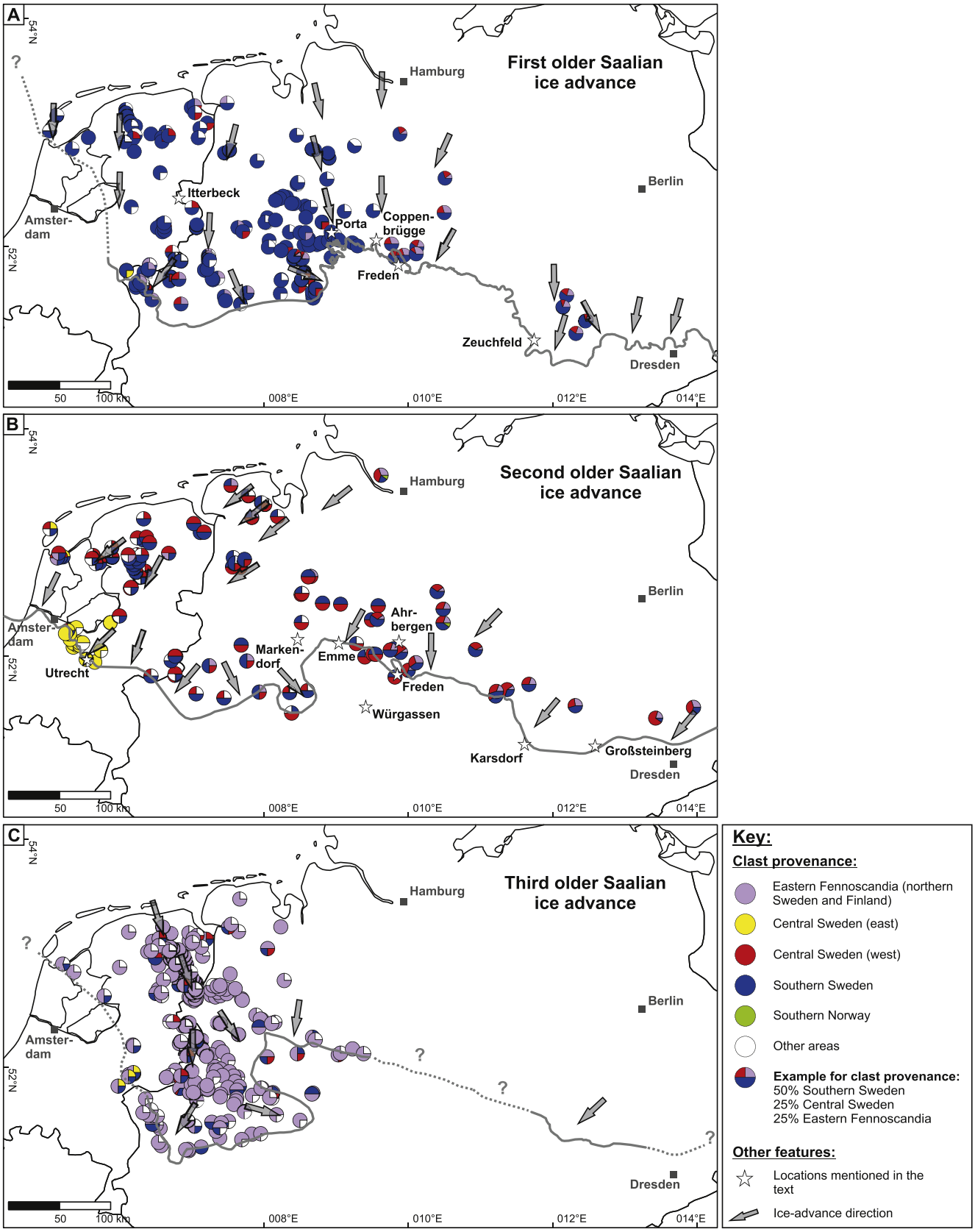

Fig. 6. Reconstruction of the older Saalian ice advances. Ice margins are based on Eissmann (1975), Skupin et al. (1993) and Ehlers et al. (2011). Clast provenance is based on Lüttig (1954, 1958), Eissmann (1975), Zandstra (1987), Skupin et al. (1993), Winter (1998), Speetzen and Zandstra (2009) and Skupin and Zandstra (2010). Data on palaeo-ice flow directions are compiled from Eissmann (1975), Ehlers and Stephan (1983, 1990), Zandstra, 1987, Höfle (1991), Skupin et al. (1993) and Skupin and Zandstra (2010). A) Maximum ice-sheet extent, clast provenance and ice-flow direction of the first older Saalian ice advance. B) Maximum ice-sheet extent, clast provenance and ice-flow direction of the second older Saalian ice advance. C) Maximum ice-sheet extent, clast provenance and ice-flow direction of the third older Saalian ice advance.

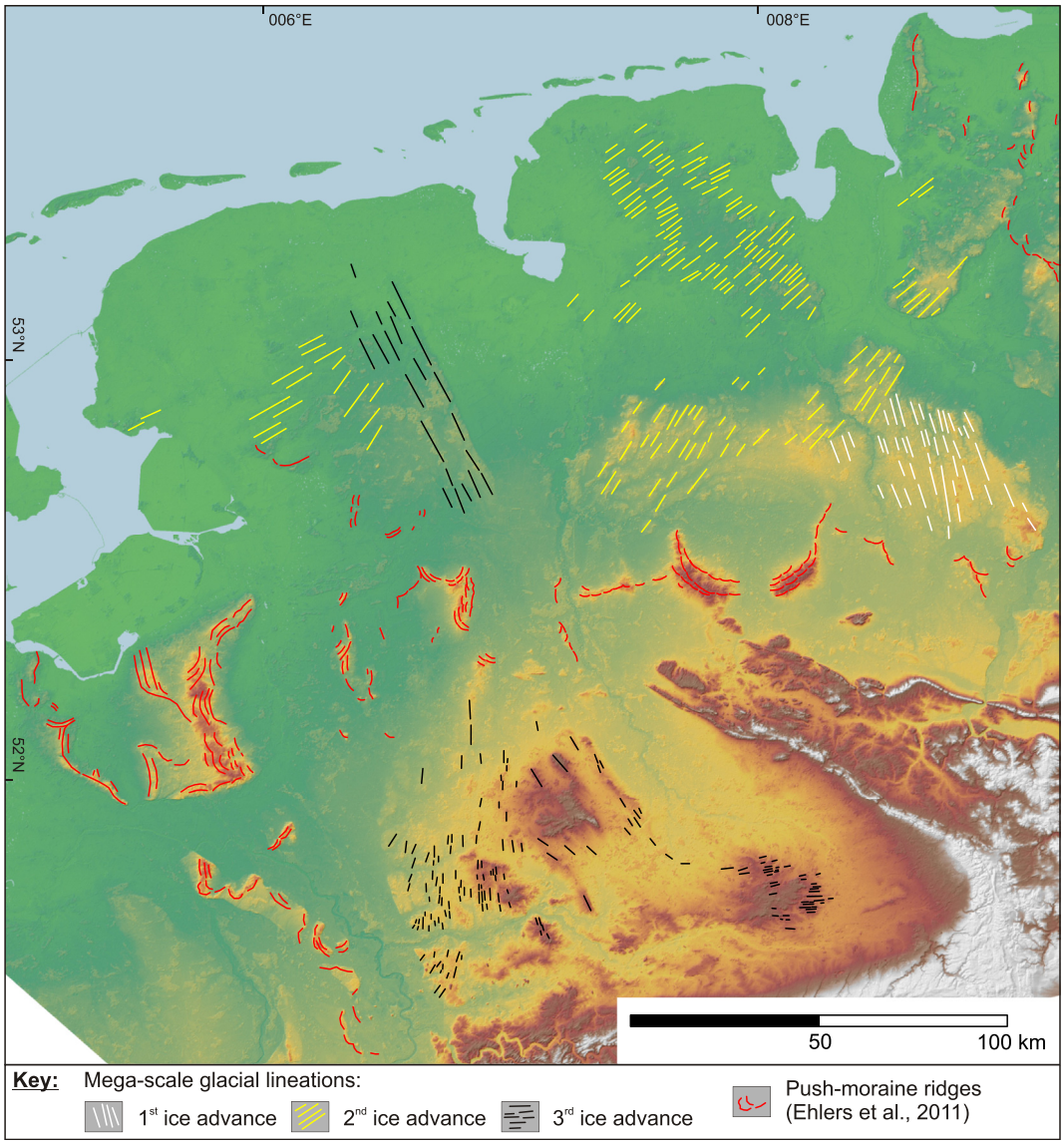

Fig. 7. Mega-scale glacial lineations mapped from the digital elevation model (EU-DEM, resolution ~30 m, vertical accuracy ~3 m) of the northwestern part of the study area. Three generations of cross-cutting mega-scale glacial lineations can be identified, corresponding to the three older Saalian ice advances.

been interpreted as glacifluvial sandurs (Ruske, 1961; Eissmann, 1975, 2002; Eissmann and Müller, 1994; Meng and Wansa, 2008), are re-interpreted as representing glacifluvial Gilbert-type deltas, based on their typical facies architecture and their vertical and lateral association with lake-bottom deposits. Lake-level highstands of approximately 180–200 m a.s.l. are indicated by deltas and lake-bottom sediments. A 190 m a.s.l. high lake level corresponds to the formation of a lake with an area of ~1777 km^2 and a volume of ~61 km^3 in the Thuringian Basin and the Unstrut and Saale valleys ("Saale-Unstrut Lake"). Several smaller lakes formed in the valleys of the Rivers Elster, Pleiße and Mulde, storing a total volume of 4 km^3 of water. The existence of a large ice-dammed lake in the Elbe valley is indicated by fine-grained lake-bottom deposits (Wolf et al., 1994).

4.1.4. Ice-sheet retreat and lake drainage

4.1.4.1. Western part of the study area (Münsterland Embayment, Weser and Leine valleys and Harz Mountains). In the Münsterland Embayment initial ice-margin retreat caused the lake to shallow and lenghten towards the west (Meinsen et al., 2011; Winsemann et al., 2016). The lake level of the Weser Lake was controlled by several overspill passes in the Teutoburger Wald Mountains, ranging in elevation between 205 and 95 m a.s.l. (Thome, 1983). These overspills were opened and closed by an ice lobe located north of the Teutoburger Wald Mountains (Thome, 1983; Winsemann et al., 2007a, 2009, 2011a, b; 2016). The opening of the overspills led to a rapid drop in lake level from ~180 to ~135 m a.s.l. (Fig. 8B; Winsemann et al., 2011a). Subsequent opening of overspills from the Münsterland Lake into the Ruhr and Emscher valleys at elevations between 105 and 40 m a.s.l. let to the drainage of 45–90 km^3 of water into the Lower Rhine Embayment and further westwards into the North Sea. Field evidence for these outburst floods is provided by flood-related deep bedrock gorges, deltas and bars in the Ruhr valley (Thome, 1983; Winsemann et al., 2016). In the Münsterland Embayment outburst-flood deposits ("Knochenkies" (bone gravel)) related to this event are preserved in the Emscher valley. In the Lower Rhine Embayment the Bönninghardt push-moraine ridge was denudated by this lake-

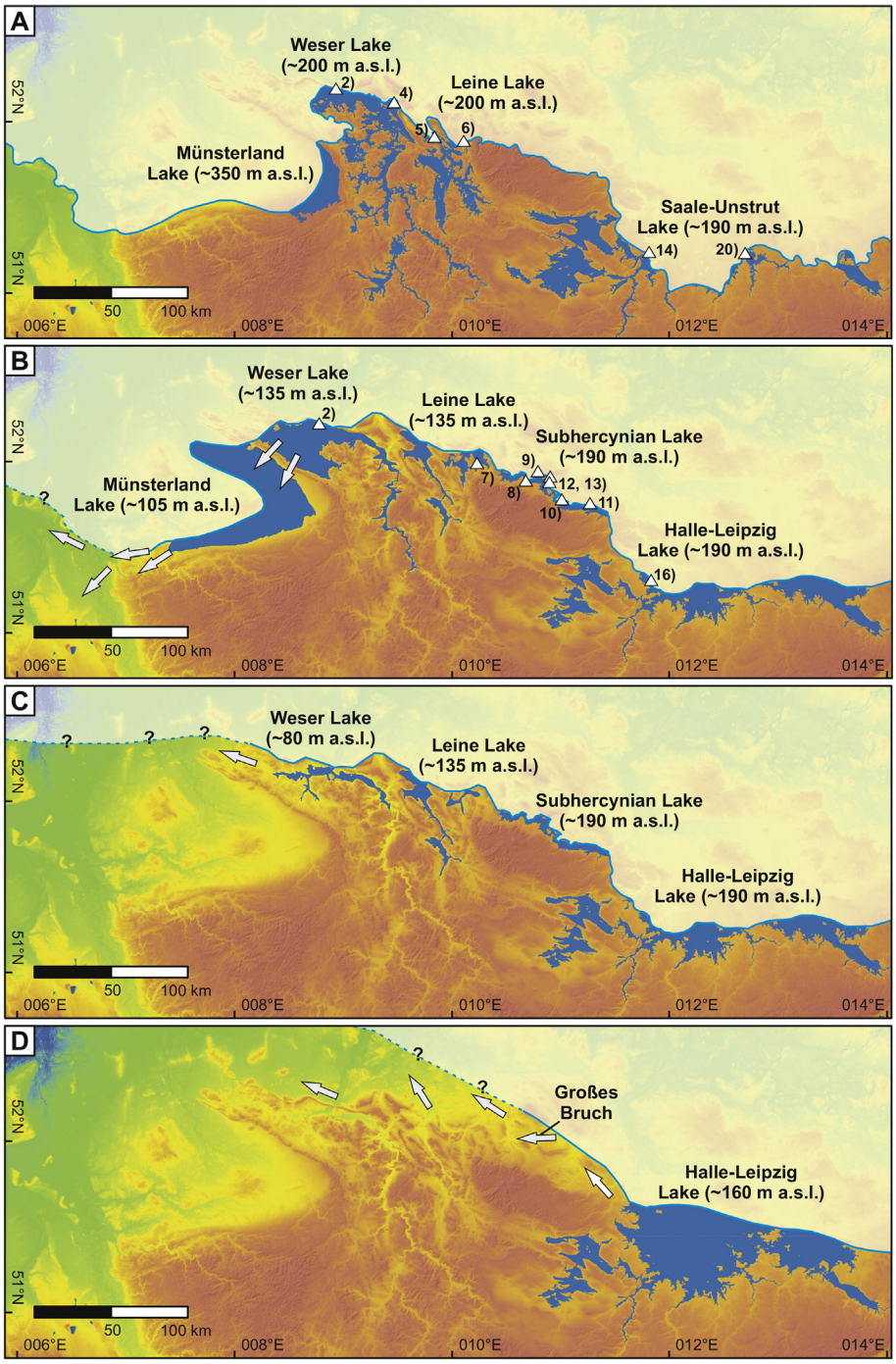

Fig. 8. Palaeogeography of ice-dammed lakes during the first ice advance of the older Saalian glaciation. Arrows indicate lake-drainage pathways. Stars indicate the sampling locations for luminescence dating. A) Maximum ice-sheet extent. B, C) Early stages of the ice-margin retreat. The lakes in the west drained mainly via the Münsterland and Lower Rhine Embayments, while the lakes in the east enlarged. D) Later stage of the retreat of the ice margin: the lakes in the west are completely drained, while the lakes in the east are connected, forming a huge lake in the Halle-Leipzig area.

outburst flood and unconformably overlain by up to 4 m thick fine-grained flood sediments derived from the Münsterland Embayment (Klostermann, 1992; Winsemann et al., 2016). The Münsterland, Weser and Leine Lakes drained completely when further ice-margin retreat opened the river valleys towards the north (Fig. 8C and D).

In the southern Subhercynian Basin in front of the Harz Mountains an ice-margin retreat of 4–14 km from the maximum extent led to the formation of a more extensive ice-dammed lake in the southern Subhercynian Basin (Fig. 8B). The palaeo-ice margin is defined by a series of isolated push-moraine ridges and bodies of ice-marginal meltwater deposits (Feldmann, 1997; Reinecke, 2006). These meltwater deposits are interpreted as glacilacustrine ice-contact deltas and subaqueous fans (Reinecke, 2006), indicating a lake level of ~190 m a.s.l. The ice-dammed lake in the Subhercynian Basin covered an area of ~340 km^2 and had a volume of ~8 km^3. The lake level in the Subhercynian Basin was controlled by the ice margin resting against a Mesozoic bedrock ridge. Passes in this

ridge have elevations of 187 and 145 m a.s.l., respectively. In front of these passes fan-shaped bodies of meltwater deposits occur at elevations between 180 and 130 m a.s.l. These deposits are interpreted as representing deposition from meltwater overspilling from the lake and thereby incising the passes. The meltwater subsequently drained via the Innerste valley towards the Leine valley. However, the age control on the glacigenic deposits in the Subhercynian Basin is very limited and a deposition of at least some of the glacilacustrine deltas and subaqueous fans during the subsequent ice advance cannot be excluded. Based on the geomorphology it is likely that ice-dammed lakes of similar extents formed during both ice advances.

4.1.4.2. Eastern part of the study area (Halle-Leipzig area and Elbe valley). An initial ice-sheet retreat of 4–25 km from the maximum extent allowed for a connection of ice-dammed lakes from the Thuringian Basin and River Unstrut valley and river valleys of the Saale, Elster, Pleiße and Mulde in the Halle-Leipzig area ("Halle-Leipzig Lake"; Fig. 8B and C). This ice-dammed lake probably evolved contemporaneously with the lake in the southern Subhercynian Basin, based on the reconstructed palaeo-ice margin (Meng and Wansa, 2008). The palaeo-ice margin is characterised by relatively continuous push- and dump-moraine ridges (Grahmann, 1925; Eissmann, 1975; Meng and Wansa, 2008). The Halle-Leipzig Lake during this stage of the ice-sheet retreat had an area of ~3326 km^2 and a volume of ~117 km^3. Towards the northwest the ice margin still rested against the easternmost parts of the Harz Mountains (Meng and Wansa, 2008), where maximum elevations of up to 250 m a.s.l. prevented the drainage of the lake.

Ongoing ice-sheet retreat allowed for the connection of the ice-dammed lakes in central Germany to form the vast Halle-Leipzig Lake (Fig. 8D), stretching from the Halle-Leipzig area and the Thuringian Basin to the Elbe valley. Deposits of the Halle-Leipzig Lake comprise widespread fine-grained glacilacustrine deposits, occurring at elevations between 79 and 155 m a.s.l. (Table 2). Based on the elevation of the potential spillways a lake level of 160 m a.s.l. is reconstructed, corresponding to an area of 6245 km^2 and a volume of 224 km^3.

Potential overspill channels of the Halle-Leipzig Lake have elevations of 150–178 m a.s.l. These overspill channels are incised into a WNW-ESE trending ridge of Palaeozoic bedrock north of Halle. Today, the bedrock ridge is dissected by the V-shaped gorge of the River Saale, which is incised by as much as 100 m to a depth of ~60 m a.s.l. (Wansa, 1997). Reconstructions of the evolution of the drainage network in this area suggest that this gorge developed during the Middle Pleistocene glaciations. While prior to the glaciations all river courses ran east of the bedrock ridge, the courses of the River Saale and its tributaries were redirected through the bedrock gorge (Schulz, 1962; Knoth, 1964; Ruske, 1963, 1973; Eissmann, 1975, 1997; Wansa, 1997). We suggest that the gorge was initially incised by flows overspilling from Elsterian ice-dammed lakes. The opening of the gorge during ice-sheet retreat probably led to sudden lake drainage and caused a lake-outburst flood. The lake-outburst flood initially followed the ice margin towards the northwest and was then deflected towards the west by higher terrain. We suggest that the lake-outburst flood was responsible for the formation of the Groβe Bruch, an east-west trending, 40 km long and 2–3 km wide channel, which is incised up to 50 m deep into Mesozoic bedrock, Palaeogene deposits and Pleistocene deposits (cf., Feldmann et al., 1997). The Groβe Bruch was previously interpreted as a subglacial tunnel valley, which formed during the maximum Saalian ice advance (Feldmann et al., 1997), or as an ice-marginal valley ("Urstromtal"), which formed during the retreat of the Saalian ice sheet (Woldstedt, 1950; Ruske, 1973; Ehlers et al., 2011). However, the geometry, width-to-depth ratio and orientation parallel to the palaeo-ice margin are rather untypical for a subglacial tunnel valley (cf., Kristensen et al., 2007; Kehew et al., 2012; Lang et al., 2012; Van der Vegt et al., 2012), but match the straight, trench-like valleys incised by glacial lake-outburst floods (cf., Baker, 1973; Carling et al., 2009a, b; Meinsen et al., 2011; Curry et al., 2014). However, the reactivation of an inherited older erosional feature by a lake-outburst flood cannot be excluded. At the western end of the Groβe Bruch the flood waters turned north, following the valley of the River Oker before spreading-out into the North German Lowlands. Erosional and depositional landforms, as isolated steep-walled incisions into bedrock and terminal fans occurring at the widening of narrow river valleys, are widespread in the assumed flood pathway and the former lake basin and are interpreted as related to the catastrophic lake drainage (cf., O'Connor, 1993; Baker, 2009; Winsemann et al., 2016).

4.2. Second older Saalian ice advance

4.2.1. Ice-flow directions and till provenance

The second ice advance into the study area commonly remained 15–25 km behind the maximum ice-sheet extent of the first older Saalian ice advance. The ice sheet extended into the western Netherlands, the Lower Rhine Embayment and the Münsterland Embayment, the valleys of Rivers Weser and Leine, the northern margin of the Harz Mountains, the Halle-Leipzig lowland area and the valley of River Elbe (Fig. 6B). The main ice-flow direction was from the northeast towards the southwest (Eissmann, 1975, 2002; Zandstra, 1987; Ehlers, 1990; Skupin et al., 1993, 2003). Till-provenance analyses show that the larger part of clasts is derived from southern Sweden (<50%) with a high proportion (>20%) of clasts from central Sweden (Zandstra, 1987; Skupin et al., 1993, 2003; Hoffmann and Meyer, 1997; Speetzen and Zandstra, 2009). Mega-scale glacial lineations related to the second ice advance in northwestern Germany and the Netherlands trend northeast to southwest (Fig. 7). This second Saalian ice advance probably corresponds to the first ice advance of the Leipzig phase in eastern Germany (Eissmann, 1975, 2002) and the second ice advance of the Drenthe advance (Freden Phase) in western Germany (Lüttig, 1954; Skupin et al., 2003).

4.2.2. Numerical ages

Luminescence ages from locations attributed to the second older Saalian ice advance suggest a correlation with MIS 6. Samples yield ages of 157 ± 16 ka for the Markendorf glacifluvial delta and 171 ± 21 to 156 ± 24 ka for the Emme glacifluvial delta at the northern margin of the Weser Lake (Table 4). Expansion-bar deposits in the upper Weser valley, which relate to the drainage of the Weser Lake, have ages of 153 ± 7 and 139 ± 8 ka (Winsemann et al., 2016). For the upper Freden glacifluvial delta (Leine Lake) luminescence ages range from 196 ± 19 to 161 ± 10 ka (Roskosch et al., 2015). In the eastern part of the study area samples yielded ages of 175 ± 10 ka for the Karsdorf glacifluvial delta in the Unstrut valley and 173 ± 19 ka for the Groβsteinberg glacifluvial delta southeast of Leipzig. The presented new age estimates are based on the median De-values except for sample Fe-2-16 from the Emme glacifluvial delta, for which the Minimum Age Model was applied (Table 4).

Lower age limits for the second ice advance are provided by glacitectonically deformed fluvial deposits of River Leine at Ahrbergen (192 ± 13 ka; Winsemann et al., 2015) and the Rhine-Maas system near Utrecht in the central Netherlands (168 ± 19 ka; Busschers et al., 2008). A younger fluvial unit from the central Netherlands, which was deposited south of the ice margin, yielded ages of 149 ± 13 to 137 ± 11 ka and is interpreted to pass laterally into glacifluvial deposits (Busschers et al., 2008). A further lower

age limit is known from the Nachtigall pit in the upper Weser valley, where an organic-rich palustrine and lacustrine succession is overlain by thin glacilacustrine deposits (Winsemann et al., 2015). ^{230}Th/U dating yielded ages of the organic-rich succession ranging from 227 + 9/-8 to 177 ± 8 ka (Waas et al., 2011).

4.2.3. Formation of ice-dammed lakes during the maximum ice extent

4.2.3.1. Western part of the study area (Münsterland Embayment, Weser and Leine valleys). The lake extent in the Münsterland Embayment during the maximum ice advance is poorly constrained by glacilacustrine deposits. Overspills into the Emscher valley have elevations of ~70 m a.s.l., indicating a lake level of ~70 m a.s.l. in the southern Münsterland Embayment. In the eastern Münsterland Embayment a maximum lake level of ~170 m a.s.l. is indicated by a potential overspill pass. In the Teutoburger Wald Mountains the ice advance closed the overspill channels at elevations of 135 m a.s.l. (cf., Winsemann et al., 2011a) (Fig. 9A). Glaciﬂuvial delta deposits were deposited at Markendorf at elevations of up to 135 m a.s.l. and at the Emme at elevations of up to 165 m a.s.l. The succession at Markendorf was subsequently transgressed by the ice as indicated by glacitectonic deformation and an overlying basal till (cf., Skupin et al., 1993, 2003; Speetzen and Wixforth, 2002). Coarse-grained lake-outburst flood deposits in the Weser valley point to a lake level of at least 170–180 m (Winsemann et al., 2016). In the Leine valley the ice margin reached approximately the same maximum extent as during the previous ice advance. Glaciﬂuvial delta deposits at Freden indicate a lake level of at least 180 m a.s.l. (Fig. 9A).

4.2.3.2. Eastern part of the study area (Halle-Leipzig area). In the eastern part of the study area ice-dammed lakes formed during the ice-sheet advance when the ice margin blocked the northwards directed drainage pathways at elevations of 178 to 150 m a.s.l. Fine-grained lake-bottom deposits, locally known as Bruckdorf clay, commonly underlie the basal till of the Leipzig phase or occur within the river valleys south of the maximum ice margin and have elevations between 105 and 160 m a.s.l. (Table 2; Eissmann, 1975, 2002). The glaciﬂuvial delta deposits near Groβsteinberg have an elevation of 155 m a.s.l. This indicates a lake level of ~160 m a.s.l. (Fig. 9A), corresponding to the formation of a lake with an area of ~2235 km^2 and a volume of ~50 km^3.

4.2.4. Ice-sheet retreat and lake drainage

4.2.4.1. Western part of the study area (Münsterland Embayment, Weser and Leine valleys). The retreat of the ice margin and opening of lake-overspill channels in the Teutoburger Wald Mountains again led to glacial lake-outburst floods, which spilled from the Weser Lake into the Münsterland Embayment (Fig. 9B), causing a lake-level fall of the Weser Lake to ~135 m a.s.l. (Meinsen et al., 2011; Winsemann et al., 2011a). Plunge pools, deep channels and streamlined hills were formed in front of the overspills and indicate that the outburst flood entered a shallow lake (Meinsen et al., 2011). The flood-related erosional features truncate the underlying till (Meinsen et al., 2011), indicating a formation after the second older Saalian ice advance, which was the last ice advance to reach this part of the Münsterland Embayment. Up to ~30 km^3 of water were temporarily stored in the northern Münsterland Embayment (Winsemann et al., 2016). Further ice-margin retreat led to the opening of the 95 m a.s.l. overspill channels in the Teutoburger Wald Mountains, releasing ~20 km^3 of water into the Münsterland Embayment. This outburst-flood event probably triggered the destabilisation of the ice lobe in the Münsterland Embayment and the opening of an outlet at 60 m a.s.l., leading to a complete drainage of the Münsterland Lake via the Lippe valley (Meinsen et al., 2011; Winsemann et al., 2016). Field evidence for this outburst flood is provided by large and deep scours at the mouth of the Lippe valley (Winsemann et al., 2016).

4.2.4.2. Eastern part of the study area (Halle-Leipzig area). The

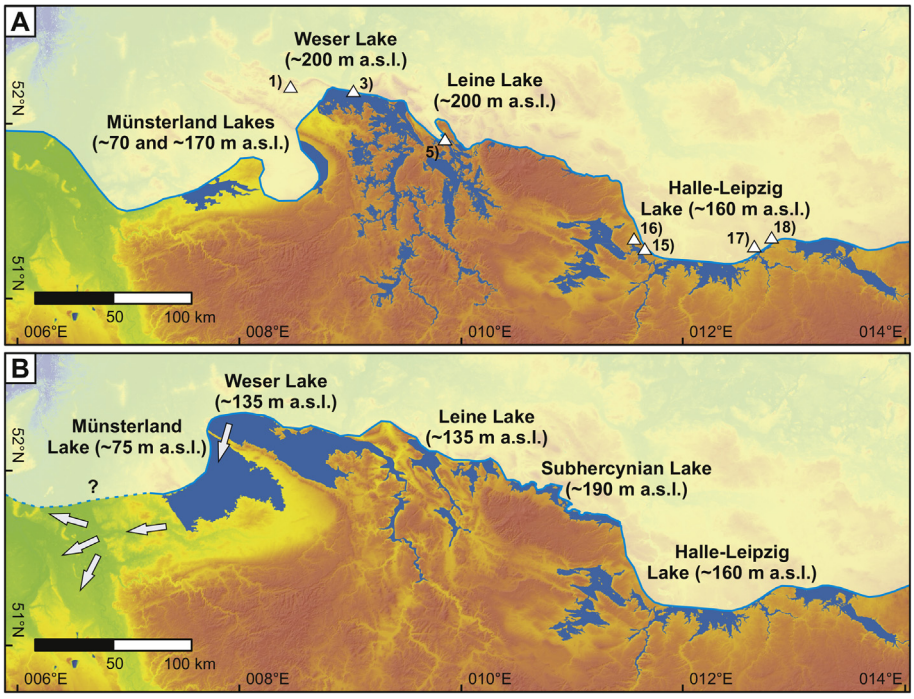

Fig. 9. Palaeogeography of ice-dammed lakes during the second ice advance of the older Saalian glaciation. Arrows indicate lake-drainage pathways. Stars indicate the sampling locations for luminescence dating. A) Maximum ice-sheet extent. B) Early stage of the ice-margin retreat: the lakes in the west drained mainly via the Münsterland and Lower Rhine Embayments, while the lakes in the east remain largely unaffected. The configuration during the later ice-margin retreat was probably similar to the first older Saalian ice advance.

retreat of the ice margin led to an increase in area and probably a shallowing of the lake. The drainage of the water stored in the lake was controlled by the ice-damming of the bedrock valley of the River Saale at elevations between 178 and 150 m a.s.l. (Fig. 9B). The opening of this bedrock valley allowed for the drainage of the lake through the Subhercynian Basin towards the northwest. The complete drainage of the Halle-Leipzig Lake would require largely ice-free conditions in the Subhercynian Basin. Due to a lack of data it is not clear if the ice-dammed lake (partly) drained at this stage or if it persisted until the third older Saalian ice advance. However, the drainage pathways towards the west were most likely still blocked by the large ice mass.

4.3. Ice streaming and minor re-advances at the end of the older Saalian glaciation

The latest stage of the older Saalian glaciation in the study area is characterised by ice streaming and/or locally restricted advances of the ice margin. In the Lower Rhine Embayment and at the southern margin of the Münsterland Embayment the maximum southwards extent of the ice margin was attained during this stage (Fig. 6C; Skupin et al., 1993; Skupin and Zandstra, 2010). The ice advanced in a narrow (~50 km) zone from the north-northwest towards the south to south-southeast and is referred to as the Hondsrug ice stream (van den Berg and Beets, 1987; Passchier et al., 2010). Till-provenance analyses show a clear dominance (>50%) of clasts derived from eastern Fennoscandia (Zandstra, 1987; Skupin et al., 1993, 2003; Speetzen and Zandstra, 2009; Skupin and Zandstra, 2010). West of the River Rhine the advance of the Hondsrug ice stream steepened push-moraine ridges (Klostermann, 1992; Skupin and Zandstra, 2010) and locally deposited till on top of successions, which had previously been partly denudated by glacial lake-outburst floods from the Weser and Münsterland Lakes (Lang and Winsemann, 2013; Winsemann et al., 2016). Mega-scale glacial lineations related to the Hondsrug ice stream in the northeastern Netherlands trend north-northwest to south-southeast, spreading radially into the Lower Rhine and Münsterland Embayments (Fig. 7). The splayed, lobate geometry of the margin of the Hondsrug ice stream (Skupin et al., 1993) indicates a termination on dry land, probably triggered by the previous catastrophic lake-drainage events (Meinsen et al., 2011; Winsemann et al., 2011a,b).

In the eastern part of the study area, the third Saalian ice advance probably corresponds to the second ice advance of the Leipzig phase and represents a minor re-advance, terminating in the Halle-Leipzig area (Fig. 6C; Eissmann, 1975, 2002). The ice-flow direction was towards the southwest and clasts have an eastern Fennoscandian to Baltic provenance (Eissmann, 1975). The re-advance of the ice sheet in the Halle-Leipzig area may have led to a new increase in lake level or to the renewed formation of an ice-dammed lake. Fine-grained lake-bottom deposits, locally known as Breitenfeld clay (Table 2), occur at elevations of 120–135 m a.s.l. (Eissmann, 1975). The formation of this lake was again controlled by the blocking of the bedrock valley of the River Saale.

4.4. Ice advances of the middle and younger Saalian (Warthe) glaciations

The middle and younger Saalian (Warthe) ice advances reached only the northeastern margin of the study area (Fig. 1; Ehlers and Stephan, 1983; Meyer, 2005; Ehlers et al., 2011). Luminescence ages of meltwater deposits range from 155 ± 21 to 130 ± 17 ka (Lüthgens et al., 2010; Kenzler et al., 2017). The ice advance direction was mainly towards the southwest and west-southwest (Ehlers and Stephan, 1983; Ehlers et al., 2011). The tills of the middle Saalian Warthe ice advance are rich in flint and Cretaceous sedimentary rocks, while tills of the younger Saalian Warthe ice advance are rich in clasts from eastern Fennoscandia (Meyer, 2005).

5. Discussion

5.1. Reliability of luminescence ages

An increasing number of luminescence ages for Middle Pleistocene successions have recently been published and the robustness of the chronologies for these deposits has greatly increased. However, there are several factors, which might lead to an age over- or underestimation. Age underestimation may be caused by anomalous fading or a natural signal close to saturation (Huntley and Lamothe, 2001; Buylaert et al., 2012; Roskosch et al., 2015; Winsemann et al., 2015). The results of our fading measurements highlight the very high signal stability of the $pIRIR_{290}$ signal. Therefore, a high signal stability and only negligible fading can be assumed for the $pIRIR_{290}$ signal.

Of more serious concern is age overestimation, which may be caused by insufficient bleaching. Insufficient bleaching may either affect the sediment itself or relate to the mixing with older material and is dependent on the depositional environment (Frechen et al., 2004; Fuchs and Owen, 2008). The obtained De-distributions (Fig. 5) suggest that insufficient bleaching has to be considered for the studied samples. However, for most samples dose residuals might have no significant impact on the natural De-values. Nevertheless, the ages presented here, which are based on the median De-values, should be regarded as maximum ages.

Glacifluvial deltas offer fair to medium conditions for the bleaching of sediments (Fuchs and Owen, 2008; Roskosch et al., 2015), depending on the flow conditions and extent of the subaerial delta plain. The sample from the sand-rich lower Freden delta (Roskosch et al., 2015) and Karsdorf delta have the lowest overdispersion values, which probably relates to a former extensive subaerial delta plain in a lower energy setting. Higher overdispersion values in other coarser-grained delta systems may primarily relate to higher flow energies and frequent re-working, leading to less suitable bleaching conditions.

The age estimates for those localities, where several samples were taken, are in good agreement (Table 4), indicating that age estimates can be regarded as reliable. Furthermore, our newly obtained results are in line with previous age estimates from other ice-marginal and fluvial deposits in the study area (Buschers et al., 2008; Roskosch et al., 2015; Winsemann et al., 2015, 2016).

5.2. Timing and regional correlation of the older Saalian ice advances

The regional correlation between the different older Saalian ice advances in northern central Europe has long remained ambiguous, especially due to the sparseness of numerical ages, and various correlations were proposed. In general, it is assumed that all Saalian ice advances, including the older, middle and younger Saalian ice advances, occurred during a single glaciation, because no interglacial deposits have been found (Caspers et al., 1995; Eissmann, 2002; Litt et al., 2007; Ehlers et al., 2011). An increasing number of new numerical ages, determined by more advanced and reliable luminescence methods (cf., Busschers et al., 2008; Kars et al., 2012; Roskosch et al., 2015; Winsemann et al., 2015), in combination with the re-evaluation of the data on ice-advance directions and clast provenance provide a detailed view on the Saalian glaciation.

Our reconstructions show that the two older Saalian ice advances reached approximately similar maximum extents, although the main ice-advance directions and source areas differed (Fig. 6). The first ice advance was characterised by an advance from the

north towards the south and a dominance of clasts derived from southern Sweden, while the second ice advance is characterised by an advance from the northeast towards the southwest and clasts are mainly derived from southern and central Sweden (Fig. 6A and B; Eissmann, 1975, 2002; Zandstra, 1987; Ehlers, 1990; Skupin et al., 1993, 2003; Ehlers et al., 2011). The two older Saalian ice advances and their deposits can thus in most locations be distinguished.

The most extensive ice advances of the Saalian glaciation have so far been correlated with MIS 6 (Lambeck et al., 2006; Litt et al., 2007; Busschers et al., 2008; Ehlers et al., 2011). Numerical ages, which indicate the correlation of the Saalian ice advances with MIS 6, were presented by Krbetschek and Stolz (1994), Preusser (1999), Busschers et al. (2008), Krbetschek et al. (2008), Roskosch et al. (2015) and Winsemann et al. (2015, 2016). Our new luminescence ages of Saalian ice-marginal deposits range from 175 ± 10 to 156 ± 24 ka and correlate with MIS 6. All new luminescence ages are from sites, which are attributed to the second older Saalian ice advance (Fig. 6B).

In addition to the widely accepted correlation of the Saalian glaciation with MIS 6, there is widespread evidence of an extensive advance of the Fennoscandian ice sheet during MIS 8 from the southern North Sea and the Netherlands (Beets et al., 2005; Meijer and Cleveringa, 2009; Laban and van der Meer, 2011), Denmark (Houmark-Nielsen, 2011), Germany (Kars et al., 2012; Roskosch et al., 2015) and southern Poland (Hall and Migoń, 2010; Lindner and Marks, 2008; Marks, 2011; Marks et al., 2016). Numerical ages supporting such an early Saalian glaciation range from ~290 to 241 ± 27 ka (Beets et al., 2005; Kars et al., 2012; Roskosch et al., 2015). Therefore, it seems possible that the first older Saalian ice advance may be older than previously thought and occurred during MIS 8.

Some regional studies provide indications for a longer time span between the first and second older Saalian ice advances. In the Lower Rhine Embayment, the Bönninghardt push-moraine ridge of the first older Saalian ice advance is denudated (Klostermann, 1992) and overlain by different generations of outburst-flood deposits (Winsemann et al., 2016), relating to the different lake-outburst floods. From the Weser and Leine valleys, Lüttig (1960) described weathering, erosion and soil formation affecting the lower till of the older Saalian glaciation (Alfeld phase). In the eastern part of the study area, a hiatus between the first (Zeitz) and second (Leipzig) Saalian till and lake-bottom sediments is widespread and characterised by a horizon of erosion and cryoturbation (Eissmann, 1975, 2002; Junge et al., 1999). Locally, this phase was also accompanied by fluvial deposition (Eissmann, 1975, 2002; Eissmann and Müller, 1994).

5.3. Impact of ice-dammed lakes on ice-margin stability

Proglacial lakes can exert an important control on ice-sheet dynamics and may cause a partial decoupling from climate trends (Stokes and Clark, 2004; Winsborrow et al., 2010; Carrivick and Tweed, 2013; Perkins and Brennand, 2015; Sejrup et al., 2016). In a steep river valley the presence of a deep lake may prevent any farther advance of ice lobes into the valley and thus constrain the ice margin to the same maximum position during multiple ice advances (Winsemann et al., 2011b; Roskosch et al., 2015). Calving losses at an ice margin in contact with a proglacial lake and an increase in the subglacial water pressure accelerate the ice flow, which lowers the ice-surface profile and may trigger ice streaming (Stokes and Clark, 2004). Rapid ice movement is also favoured by a low permeability substratum, as fine-grained lake-bottom deposits, which allow for meltwater pressure to build-up, ice-bed decoupling and enhanced basal sliding (Hoffmann and Piotrowski, 2001). The formation of the Hondsrug ice stream in the Netherlands and northwest Germany, which was the last ice advance to reach the western part of the study area (Figs. 6C and 7; cf., van den Berg and Beets, 1987; Skupin et al., 1993; Passchier et al., 2010), was probably initiated by lake drainage and associated enhanced ice draw-down in the Münsterland and Lower Rhine Embayments (Meinsen et al., 2011; Winsemann et al., 2011b). The flow direction of the Hondsrug ice stream was probably controlled by the presence of a stagnant ice lobe further west, the lithology of the substratum and a zone of increased geothermal heat flow in the southern North Sea and the eastern Netherlands (van den Berg and Beets, 1987; Bregman and Smit, 2012; Cohen et al., 2017).

5.4. Evolution of the major meltwater-drainage pathways

The analysis of the distribution of glacilacustrine deposits and lake spillways clearly indicates the presence of extensive and deep ice-dammed lakes. The lake levels ranged from 350 to 180 m a.s.l. during the maximum extent and 190 to 70 m a.s.l. during the retreat of the Saalian ice sheets (Figs. 8 and 9). Lakes attained maximum depths of up to ~150 m. Lake overspill channels, connecting the individual lakes, allowed for an interaction of the lake levels. The retreat of the ice margin caused the successive drainage of the lakes.

The drainage of the meltwater along the southwestern margin of the Middle Pleistocene Saalian ice sheets (Fig. 10) was controlled by the proglacial lakes dammed in river valleys and lowland areas from the Münsterland Embayment in the west to the drainage divide between the Atlantic and the Black Sea in eastern Poland (Carpathians). The location and extent of these lakes depended on local topography and the presence of ice dams, while the final drainage of the stored meltwater also depended on the ice dams blocking the drainage towards the west. Our reconstruction indicates the existence of connections between the different lakes via overspill channels, leading to an interaction between the lake levels in the individual lakes. The restoration of the drainage routes towards the west and northwest required the successive opening of all ice dams and the drainage of the proglacial lakes. Major drainage pathways are characterised by trench-like valleys, which are up to 3 km wide and 50 m deep (e.g., Großes Bruch).

The drainage of the Fennoscandian ice sheets is also recorded in deep marine deposits in the Atlantic, which was connected to the drainage system of the ice sheets via the English Channel palaeo-river system (Fig. 10) during sea-level lowstand (Gupta et al., 2007, 2017; Toucanne et al., 2009a, b; Collier et al., 2015). The discharge was very high at ~455 ka (MIS 12), ~160-150 ka (MIS 6) and ~25-15 ka (MIS 2), while less intense discharge events occurred at ~345-335 ka (MIS 10), ~275-265 ka (MIS 8; Toucanne et al., 2009a, b). The discharge of the English Channel palaeo-river was probably controlled by the coalescence of the Fennoscandian and the British Islands ice sheets in the northern North Sea, preventing the northwards drainage of meltwater via the North Sea into the North Atlantic (Toucanne et al., 2009a, b). The coalescence of the Saalian ice sheets caused the formation of an extensive ice-dammed lake in the southern North Sea basin (Fig. 10). The depositional record of the Saalian North Sea Lake comprises fine-grained glacilacustrine deposits and delta-topset deposits related to the Rhine-Meuse system ("Unit S4"; Busschers et al., 2008).

The initial opening of the English Channel and the initiation of the palaeo-river system was probably triggered by a glacial lake-outburst flood from the North Sea Lake during MIS 12 (Gibbard, 2007; Gupta et al., 2007, 2017; Toucanne et al., 2009a, b; Collier et al., 2015). Lower discharges may indicate that no coalescence of the Fennoscandian and the British Islands ice sheets existed during MIS10 and MIS 8 and the main meltwater drainage occurred via the northern North Sea (Toucanne et al., 2009a, b). The extent of

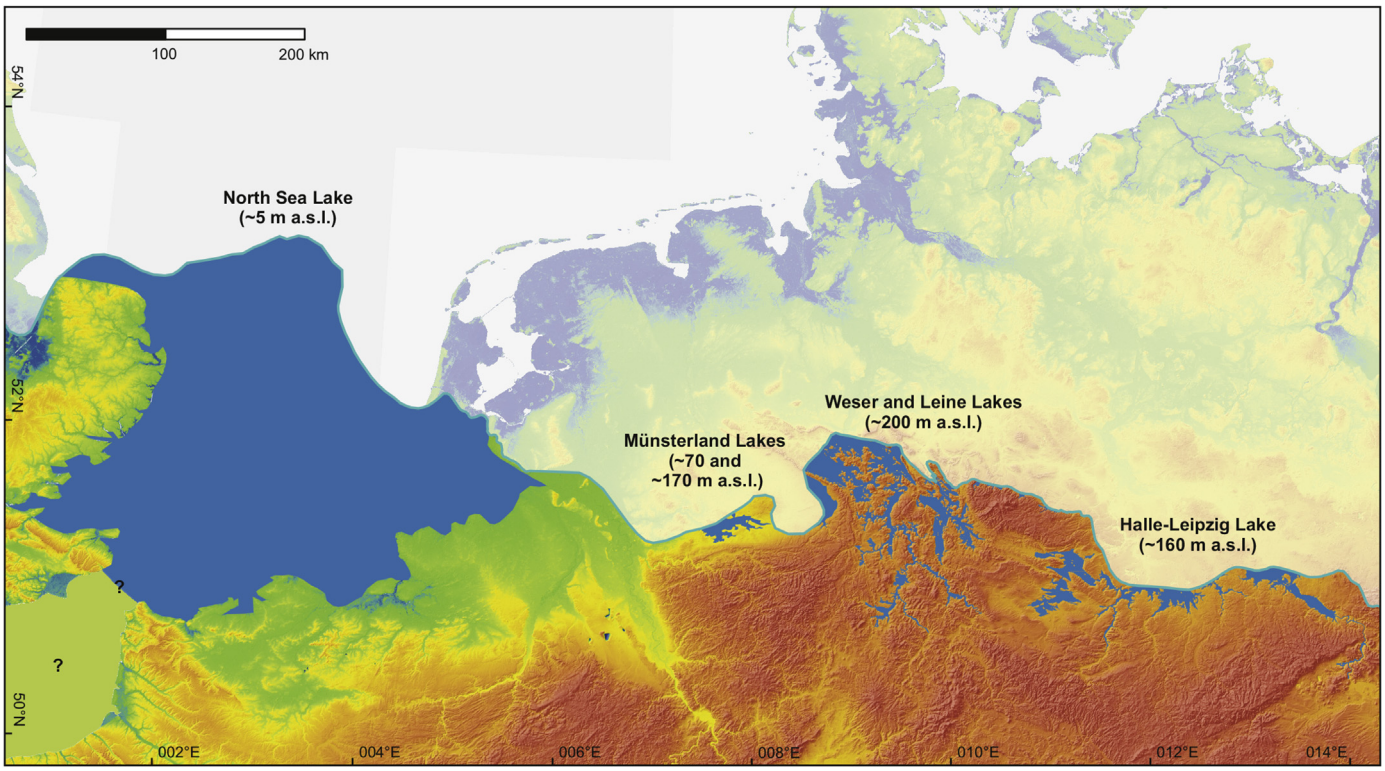

Fig. 10. Palaeogeography and large-scale drainage pattern during the second older Saalian ice advance, representing the maximum ice-sheet extent in the west. The extend of the North Sea Lake is modified from Busschers et al. (2008) and Cohen et al. (2017).

these ice sheets in the North Sea basin was probably less than during the subsequent MIS 6 ice advance (Fig. 6A and B). New reconstructions of the ice margin in the southern North Sea suggest a connection of ice lobes between eastern England, the southern North Sea and the Netherlands (Graham et al., 2011; White et al., 2017). Therefore, the Saalian North Sea Lake was probably able to store larger volumes of meltwater, which largely drained towards the north during deglaciation. The phase of palaeo-river activity at ~275-265 ka may correlate with an earlier Saalian ice advance in northern central Europe during MIS 8. However, a correlation with MIS 8 must be supported by additional numerical dates from glacigenic deposits.

Two distinct phases of palaeo-river activity are recorded for MIS 6, the first phase occurring around 170 to 160 ka and the second, more intense phase around 150 ka (Penaud et al., 2009). These two phases may correspond to the second ice-sheet advance during MIS 6 and the following phase of ice decay, subsequent re-advance and ice streaming (third ice advance). Large volumes of meltwater were probably only released during the onset of the final deglaciation (Penaud et al., 2009; Toucanne et al., 2009b). During the subsequent Warthe ice advances the discharge was low, because lesser ice-sheet extents allowed for the meltwater to drain northwards via the northern North Sea into the Atlantic (Toucanne et al., 2009a, b).

6. Conclusions

We present a comprehensive palaeogeographic reconstruction for the Middle Pleistocene older Saalian glaciation and related proglacial lakes in northern central Europe. The reconstruction is based on the integration of geomorphologic features, facies analysis, till provenance, ice-flow direction and numerical ages. Our results indicate two major ice advances, which reached very similar maximum extents but differ in the main ice-advance directions and till provenance.

The first older Saalian ice advance was characterised by an ice advance from the north towards the south and a dominance of clasts derived from southern Sweden. Luminescence ages for this first older Saalian ice advance are sparse, but may point to an ice advance during MIS 8 or early MIS 6 (e.g., Beets et al., 2005; Kars et al., 2012; Roskosch et al., 2015).

The second older Saalian ice advance was initially characterised by an ice advance from the northeast towards the southwest. Clasts are mainly derived from southern and central Sweden. New luminescence ages from ice-marginal deposits of this second older Saalian ice advance range from 175 ± 10 to 156 ± 24 ka. The latest stage of the older Saalian ice advance in the study area (third ice advance) was characterised by ice streaming (Hondsrug ice stream) in the west and a re-advance in the east. Clasts of this stage are mainly derived from eastern Fennoscandia.

The advancing ice sheets repeatedly blocked northwards directed drainage pathways and led to the formation of extensive ice-dammed lakes, storing up to 265 km^3 of water in four larger and several smaller lakes during the maximum ice-sheet extent. Because the formation of lakes was mainly controlled by ice-damming at bedrock spillways, the lake levels and extends were probably very similar throughout the repeated ice advances. The retreat of the ice margin changed the lake configuration and opened lake overspills, leading to a successive drainage of the lakes. Catastrophic lake-drainage events occurred when large overspills were suddenly opened.

The middle and younger Saalian (Warthe) ice advances, which occurred at 155 ± 21 to 130 ± 17 ka (Lüthgens et al., 2010; Kenzler et al., 2017), reached only the northeastern margin of the study area. The ice advance direction was mainly towards the southwest and west-southwest (Ehlers et al., 2011). The tills of the middle

Saalian Warthe ice advance are rich in flint and Cretaceous sedimentary rocks, while tills of the younger Saalian Warthe ice advance are rich in clasts from eastern Fennoscandia (Meyer, 2005).

Acknowledgements

Funding for this study was provided in the framework of the "Wege in die Forschung" program by Leibniz Universität Hannover (project title: "Mittelpleistozäne Megafluten in Norddeutschland: Auswirkungen und Magnituden"; Grant No. II-05-2014-05). We would like to thank S. Hesse for preparation of OSL samples. F. Busch, J. Sievers and T. Steinbrecher are thanked for GIS work. The hill-shaded relief maps were produced using Copernicus data and information funded by the European Union (EU-DEM layers) and data provided by the Bezirksregierung Köln. K. Cohen, W. Bartholomäus, B.-C. Ehling, M. Frechen, K. Skupin, E. Speetzen and S. Wansa are thanked for discussion. The constructive comments of two anonymous reviewers are appreciated and helped to improve the manuscript.

References

Baker, V.R., 1973. Paleohydrology and sedimentology of lake missoula flooding in Eastern Washington. Boulder. CO. Geol. Soc. Am. Special Pap. 144, 1–7.
Baker, V.R., 2009. Channelled scabland morphology. In: Burr, D.M., Carling, P.A., Baker, V.R. (Eds.), Megaflooding on Earth and Mars. Cambridge University Press, Cambridge, pp. 65–77.
Beets, C.J., Beets, D.J., 2003. A high resolution stable isotope record of the penultimate deglaciation in lake sediments below the city of Amsterdam, The Netherlands. Quat. Sci. Rev. 22, 195–207.
Beets, D.J., Meijer, T., Beets, C.J., Cleveringa, P., Laban, C., Van der Spek, A.J.F., 2005. Evidence for a middle Pleistocene glaciation of MIS 8 age in the southern North Sea. Quat. Int. 133, 7–19.
Bettenstaedt, F., 1934. Stauseebildung und Vorstoß des diluvialen Inlandeises in seinem Randbereich bei Halle a. S. Jahrb. Hallescher Verband N. F. 13, 241–313.
Böse, M., Lüthgens, C., Lee, J.R., Rose, J., 2012. Quaternary glaciations of northern Europe. Quat. Sci. Rev. 44, 1–25.
Boulton, G.S., Dongelmans, P., Punkari, M., Broadgate, M., 2001. Palaeoglaciology of an ice sheet through a glacial cycle: the European ice sheet through the Weichselian. Quat. Sci. Rev. 20, 591–625.
Bregman, E.P.H., Smit, F.W.H., 2012. Genesis of the Hondsrug, a Saalian Megaflute, Drenthe, the Netherlands. European Geopark de Hondsrug, Borger, 123 pp.
Brouard, E., Lajeunesse, P., Cousineau, P.A., Govare, É., Locat, J., 2016. Late Wisconsinan deglaciation and proglacial lakes development in the Charlevoix region, southeastern Québec, Canada. Boreas 45, 754–772.
Busschers, F.S., Van Balen, R.T., Cohen, K.M., Kasse, C., Weerts, H.J., Wallinga, J., Bunnik, F.P., 2008. Response of the Rhine–Meuse fluvial system to Saalian ice-sheet dynamics. Boreas 37, 377–398.
Buylaert, J.P., Murray, A.S., Thomsen, K.J., Jain, M., 2009. Testing the potential of an elevated temperature IRSL signal from K-feldspar. Radiat. Meas. 44, 560–565.
Buylaert, J.-P., Jain, M., Murray, A.S., Thomsen, K.J., Thiel, C., Sohbati, R., 2012. A robust feldspar luminescence dating method for Middle and Late Pleistocene sediments. Boreas 41, 435–451.
Carling, P.A., 2013. Freshwater megaflood sedimentation: what can we learn about generic processes? Earth Sci. Rev. 125, 87–113.
Carling, P.A., Burr, D.M., Johnsen, T.F., Brennand, T.A., 2009a. A review of open-channel megaflood depositional landforms on Earth and Mars. In: Burr, D.M., Carling, P.A., Baker, V.R. (Eds.), Megaflooding on Earth and Mars. Cambridge University Press, Cambridge, pp. 33–49.
Carling, P.A., Herget, J., Lanz, J.K., Richardson, K., Pacifici, A., 2009b. Channel-scale erosional bedforms in bedrock and in loose granular material: character, processes and implications. In: Burr, D.M., Carling, P.A., Baker, V.R. (Eds.), Megaflooding on Earth and Mars. Cambridge University Press, Cambridge, pp. 13–32.
Carrivick, J.L., Tweed, F.S., 2013. Proglacial lakes: character, behaviour and geological importance. Quat. Sci. Rev. 78, 34–52.
Caspers, G., Jordan, H., Merkt, J., Meyer, K.-D., Müller, H., Streif, H., 1995. Niedersachsen. In: Benda, L. (Ed.), Das Quartär Deutschlands. Bornträger, Berlin, pp. 23–58.
Clark, C.D., 1993. Mega-scale glacial lineations and cross-cutting ice-flow landforms. Earth Surf. Process. landforms 18, 1–29.
Cohen, K.M., Gibbard, P.L., Weerts, H.J.T., 2014. North Sea palaeogeographical reconstructions for the last 1 Ma. Neth. J. Geosci. 93, 7–29.
Cohen, K.M., Westley, K., Erkens, G., Hijma, M.P., Weerts, H.J.T., 2017. The North Sea. In: Flemming, N.C., Harff, J., Moura, D., Burgess, A., Bailey, G.N. (Eds.), Submerged Landscapes of the European Continental Shelf: Quaternary Palaeoenvironments. Wiley, Chichester, pp. 147–186.
Colarossi, D., Duller, G.A.T., Roberts, H.M., Tooth, S., Lyons, R., 2015. Comparison of paired quartz and feldspar post-IR IRSL dose distributions in poorly bleached fluvial sediments from South Africa. Quat. Geochronol. 30, 233–238.
Collier, J.S., Oggioni, F., Gupta, S., García-Moreno, D., Trentesaux, A., De Batist, M., 2015. Streamlined islands and the English Channel megaflood hypothesis. Glob. Planet. Change 135, 190–206.
Curry, B.B., Hajic, E.R., Clark, J.A., Befus, K.M., Carrell, J.E., Brown, S.E., 2014. The Kankakee torrent and other large meltwater flooding events during the last deglaciation, Illinois, USA. Quat. Sci. Rev. 90, 22–36.
Ehlers, J., 1990. Reconstructing the dynamics of the north-west European Pleistocene ice sheets. Quat. Sci. Rev. 9, 71–83.
Ehlers, J., Stephan, H.-J., 1983. Till fabric and ice-movement. In: Ehlers, J. (Ed.), Glacial Deposits in North-west Europe. Balkema, Rotterdam, pp. 267–274.
Ehlers, J., Eissmann, L., Lippstreu, L., Stephan, H.J., Wansa, S., 2004. Pleistocene glaciations of north Germany. In: Ehlers, J., Gibbard, P.L. (Eds.), Quaternary Glaciations - Extent and Chronology. Part 1. Europe. Developments in Quaternary Sciences 2. Elsevier, Amsterdam, pp. 135–146.
Ehlers, J., Grube, A., Stephan, H.J., Wansa, S., 2011. Pleistocene glaciations of North Germany – new results. In: Ehlers, J., Gibbard, P.L., Hughes, P.D. (Eds.), Quaternary Glaciations – Extent and Chronology – a Closer Look. Developments in Quaternary Science 15. Elsevier, Amsterdam, pp. 149–162.
Eissmann, L., 1975. Das Quartär der Leipziger Tieflandsbucht und angrenzender Gebiete um Saale und Elbe – modell einer Landschaftsentwicklung am Rand der europäischen Kontinentalvereisung. Schriftenr. Geol. Wiss. 2, 1–263.
Eissmann, L., 1994. Grundzüge der Quartärgeologie Mitteldeutschlands. Altenbg. Naturwiss. Forsch. 7, 55–136.
Eissmann, L., 1997. Das quartäre Eisszeitalter in Sachsen und Nordostthüringen. Altenbg. Naturwiss. Forsch. 8, 1–98.
Eissmann, L., 2002. Quaternary geology of eastern Germany (saxony, saxon–Anhalt, south Brandenburg, Thüringia), type area of the Elsterian and saalian stages in Europe. Quat. Sci. Rev. 21, 1275–1346.
Eissmann, L., Müller, A., 1994. Gedenkexkursion 150 Jahre Inlandeistheorie in Sachsen. Flussterrassen, Endmoränen und Gletscherschliffe in Nordwestsachsen. Altenbg. Naturwiss. Forsch. 7, 378–430.
Fehrentz, M., Radtke, U., 2001. Luminescence dating of Pleistocene outwash sediments of the Senne area (Eastern Münsterland, Germany). Quat. Sci. Rev. 20, 725–729.
Feldmann, L., 1997. Drenthezeitliche Eisrandlagen zwischen Harz und Allertal. Z. für Geol. Wiss. 25, 181–190.
Feldmann, L., Meyer, K.-D., 1998. Quartär in Niedersachsen. Exkursionsführer zur Jubiläums-Hauptversammlung der Deutschen Quartärvereinigung in Hannover. Exkursion B, Deuqua, Hannover, 205 pp.
Feldmann, L., Groetzner, J.-P., Weymann, H.-J., 1997. Zur pleistozänen Geschichte des „Großen Bruchs" im Nördlichen Harzvorland. Geol. Beiträge Hann. 2, 127–137.
Frechen, M., Schwab, M.J., Sutter, I., 2004. Luminescence and radiocarbon dating of lake sediments from east Antarctica. In: Higham, T., Bronk Ramsey, C., Owen, C. (Eds.), Radiocarbon and Archaeology. Oxbow Books, Oxford, pp. 17–34.
Frouin, M., Huot, S., Kreutzer, S., Lahaye, C., Lamothe, M., Philippe, A., Mercier, N., 2017. An improved radiofluorescence single-aliquot regenerative dose protocol for K-feldspars. Quat. Geochronol. 38, 13–24.
Fuchs, M., Owen, L.A., 2008. Luminescence dating of glacial and associated sediments: review, recommendations and future directions. Boreas 37, 636–659.
Galbraith, R.F., Roberts, R.G., Laslett, G.M., Yoshida, H., Olley, J.M., 1999. Optical dating of single and multiple grains of quartz from Jinmium rock shelter, northern Australia: Part I, experimental design and statistical models. Archaeometry 41, 339–364.
Gassert, D., 1975. Stausee-und Rinnenbildung an den südlichsten Eisrandlagen in Norddeutschland. Würzburger Geographische Arbeiten 43, 55–65.
Gibbard, P.L., 2007. Palaeogeography: Europe cut adrift. Nature 448, 259–260.
Gibbard, P., Cohen, K.M., 2008. Global chronostratigraphical correlation table for the last 2.7 million years. Episodes 31, 243–247.
Gorlach, A., Hang, T., Kalm, V., 2017. GIS-based reconstruction of Late Weichselian proglacial lakes in northwestern Russia and Belarus. Boreas. https://doi.org/10.1111/bor.12223.
Graham, A.G., Stoker, M.S., Lonergan, L., Bradwell, T., Stewart, M.A., 2011. The Pleistocene glaciations of the North Sea basin. In: Ehlers, J., Gibbard, P.L., Hughes, P.D. (Eds.), Quaternary Glaciations – Extent and Chronology – a Closer Look. Developments in Quaternary Science 15. Elsevier, Amsterdam, pp. 261–278.
Grahmann, R., 1925. Diluvium und Pliozän in Nordwestsachsen. Abh. sächsischen Akad. Wiss. 39, 1–82.
Grahmann, R., 1929. Geologische Karte von Sachsen, 1:25,000, Blatt 4646, Colmnitz. Sächsisches Geologisches Landesamt, Leipzig.
Grahmann, R., Kossmat, F., 1927. Geologische Karte von Sachsen, 1:25,000, Blatt 4645, Riesa-Strehla. Sächsisches Geologisches Landesamt, Leipzig.
Guérin, G., Mercier, N., 2011. Determining gamma dose rates by field gamma spectroscopy in sedimentary media: results of Monte Carlo simulations. Radiat. Meas. 46, 190–195.
Gupta, S., Collier, J.S., Palmer-Felgate, A., Potter, G., 2007. Catastrophic flooding origin of shelf valley systems in the English Channel. Nature 448, 342–345.
Gupta, S., Collier, J.S., Garcia-Moreno, D., Oggioni, F., Trentesaux, A., Vanneste, K., De Batst, M., Camelbeeck, T., Potter, G., van Vliet-Lanoë, B., Arthur, J.C., 2017. Two-stage opening of the dover strait and the origin of island Britain. Nat. Commun. 8 https://doi.org/10.1038/ncomms15101.
Hall, A.M., Migoń, P., 2010. The first stages of erosion by ice sheets: evidence from central Europe. Geomorphology 123, 349–363.
Hambrey, M., 1995. Glacial Environments. UCL Press, London, 296 pp.

Härtel, F., 1941. Geologische Karte von Sachsen, 1:25,000, Blatt 4748, Radeburg. Reichsstelle für Bodenforschung, Leipzig.
Herget, J., 1998. Temporäre Entwässerungsbahnen am Südrand der Westfälischen Tieflandsbucht – ein Szenario. In: Glatthaar, D., Herget, J. (Eds.), Physische Geographie und Landeskunde – Festschrift für Herbert Liedtke. Bochumer Geographische Arbeiten, Sonderreihe 13. Geographisches Institut, Bochum, pp. 23–30.
Hoffmann, K., Meyer, K.-D., 1997. Leitgeschiebezählungen von elster- und saalezeitlichen Ablagerungen aus Sachsen, Sachsen-Anhalt und dem östlichen Niedersachsen. Leipz. Geowiss. 5, 115–128.
Hoffmann, K., Piotrowski, J.A., 2001. Till melange at Amsdorf, central Germany: sediment erosion, transport and deposition in a complex, soft-bedded subglacial system. Sediment. Geol. 140, 215–234.
Hornung, J.J., Asprion, U., Winsemann, J., 2007. Jet-efflux deposits of a subaqueous ice-contact fan, glacial Lake Rinteln, northwestern Germany. Sediment. Geol. 193, 167–192.
Höfle, H.-C., 1991. Über die interne Struktur und die stratigraphische Stellung mehrerer Endmoränenwälle im Bereich der Nordheide bis östlich Lüneburg. Geol. Jahrb. A 126, 151–169.
Houmark-Nielsen, M., 2011. Pleistocene glaciations in Denmark: a closer look at chronology, ice dynamics and landforms. In: Ehlers, J., Gibbard, P.L., Hughes, P.D. (Eds.), Quaternary Glaciations – Extent and Chronology – a Closer Look. Developments in Quaternary Science 15. Elsevier, Amsterdam, pp. 47–58.
Huhle, K., 2015. Lithostratigrafie einiger Bohrungen in der Dresdner Elbtalwanne. Geol. Saxonica 60, 461–488.
Huntley, D.J., Baril, M.R., 1997. The K content of the K-feldspars being measured in optical dating or thermoluminescence dating. Anc. TL 15, 11–13.
Huntley, D.J., Lamothe, M., 2001. Ubiquity of anomalous fading in K-feldspars and the measurement and correction for it in optical dating. Can. J. Earth Sci. 38, 1093–1106.
Junge, F.W., 1998. Die Bändertone Mitteldeutschlands und angrenzender Gebiete. Altenbg. Naturwiss. Forsch. 9, 1–210.
Junge, F.W., Böttger, T., Siegert, C., 1999. Die Stauseesedimente des Bruckdorfer Horizontes: ergebnis der Eisrandoszillation des saaleglazialen skandinavischen Inlandeises in Mitteldeutschland. Mauritiana 17, 257–276.
Kars, R.H., Wallinga, J., Cohen, K.M., 2008. A new approach towards anomalous fading correction for feldspar IRSL dating – tests on samples in field saturation. Radiat. Meas. 43, 786–790.
Kars, R.H., Busschers, F.S., Wallinga, J., 2012. Validating post IR-IRSL dating on K-feldspars through comparison with quartz OSL ages. Quat. Geochronol. 12, 74–86.
Kehew, A.E., Lord, M.L., 1986. Origin and large-scale erosional features of glacial-lake spillways in the northern Great Plains. Geol. Soc. Am. Bull. 97, 162–177.
Kehew, A.E., Piotrowski, J.A., Jørgensen, F., 2012. Tunnel valleys: concepts and controversies – a review. Earth Sci. Rev. 113, 33–58.
Kenzler, M., Tsukamoto, S., Meng, S., Frechen, M., Hüneke, H., 2017. New age constraints from the SW Baltic Sea area—implications for Scandinavian Ice Sheet dynamics and palaeo-environmental conditions during MIS 3 and early MIS 2. Boreas 46, 34–52.
Klostermann, J., 1992. Das Quartär der Niederrheinischen Bucht – Ablagerungen der letzten Eiszeit am Niederrhein. Geologisches Landesamt Nordrhein-Westfalen, Krefeld, 200 pp.
Knoth, W., 1964. Zur Kenntnis der pleistozänen Mittelterrassen der Saale und Mulde nördlich von Halle. Geologie 13, 598–616.
Krbetschek, M.R., Stolz, W., 1994. Lumineszenz-Datierungen aus pleistozänen Sedimenten aus Tagebauen des mitteldeutschen und lausitzer Braunkohlereviers. Altenbg. Naturwiss. Forsch. 7, 289–295.
Krbetschek, M.R., Degering, D., Alexowsky, W., 2008. Infrarot-Radiofluoreszenz-Alter (IR-RF) unter-saalezeitlicher Sedimente Mittel-und Ostdeutschlands. Z. Dtsch. Ges. für Geowiss. 159, 133–140.
Kreutzer, S., Lauer, T., Meszner, S., Krbetschek, M.R., Faust, D., Fuchs, M., 2014a. Chronology of the Quaternary profile Zeuchfeld in Saxony-Anhalt/Germany – a preliminary luminescence dating study. Zeitschrift für Geomorphologie. Suppl. Issues 58, 5–26.
Kreutzer, S., Schmidt, C., DeWitt, R., Fuchs, M., 2014b. The a-value of polymineral fine grain samples measured with the post-IR IRSL protocol. Radiat. Meas. 69, 18–29.
Kristensen, T.B., Huuse, M., Piotrowski, J.A., Clausen, O.R., 2007. A morphometric analysis of tunnel valleys in the eastern North Sea based on 3D seismic data. J. Quat. Sci. 22, 801–815.
Laban, C., van der Meer, J.J., 2011. Pleistocene glaciation in The Netherlands. In: Ehlers, J., Gibbard, P.L., Hughes, P.D. (Eds.), Quaternary Glaciations – Extent and Chronology – a Closer Look. Developments in Quaternary Science 15. Elsevier, Amsterdam, pp. 247–260.
Lang, J., Winsemann, J., 2013. Lateral and vertical facies relationships of bedforms deposited by aggrading supercritical flows: from cyclic steps to humpback dunes. Sediment. Geol. 296, 36–54.
Lang, J., Winsemann, J., Steinmetz, D., Polom, U., Pollok, L., Böhner, U., Serangeli, J., Brandes, C., Hampel, A., Winghart, S., 2012. The Pleistocene of Schöningen, Germany: a complex tunnel valley fill revealed from 3D subsurface modelling and shear wave seismics. Quat. Sci. Rev. 39, 86–105.
Lambeck, K., Purcell, A., Funder, S., Kjær, K., Larsen, E., Moller, P., 2006. Constraints on the Late Saalian to early Middle Weichselian ice sheet of Eurasia from field data and rebound modelling. Boreas 35, 539–575.
LaRocque, A., Dubois, J.M.M., Leblon, B., 2003. A methodology to reconstruct small and short-lived ice-dammed lakes in the Appalachians of Southern Québec. Quat. Int. 99, 59–71.
Lauer, T., Krbetschek, M., Mauz, B., Frechen, M., 2012. Yellow stimulated luminescence from potassium feldspar: observations on its suitability for dating. Radiat. Meas. 47, 974–980.
Lee, J.R., Busschers, F.S., Sejrup, H.P., 2012. Pre-Weichselian Quaternary glaciations of the British Isles, The Netherlands, Norway and adjacent marine areas south of 68°N: implications for long-term ice sheet development in northern Europe. Quat. Sci. Rev. 44, 213–228.
Li, B., Li, S.-H., 2011. Luminescence dating of K-feldspar from sediments: a protocol without anomalous fading correction. Quat. Geochronol. 6, 468–479.
Lindner, L., Marks, L., 2008. Pleistocene stratigraphy of Poland and its correlation with stratotype sections in the Volhynian Upland (Ukraine). Geochronometria 31, 31–37.
Litt, T., Behre, K.-E., Meyer, K.-D., Stephan, H.-J., Wansa, S., 2007. Stratigraphische Begriffe für das Quartär des norddeutschen Vereisungsgebietes. E&G Quat. Sci. J. 56, 7–65.
Litt, T., Schmincke, H.-U., Frechen, M., Schlüchter, C., 2008. Quaternary. In: McCann, T. (Ed.), The Geology of Central Europe, Mesozoic and Cenozoic, vol. 2. Geological Society, London, pp. 1287–1340.
Lønne, I., 1995. Sedimentary facies and depositional architecture of ice-contact glaciomarine systems. Sediment. Geol. 98, 13–43.
Lüthgens, C., Böse, M., Krbetschek, M., 2010. On the age of the young morainic morphology in the area ascribed to the maximum extent of the Weichselian glaciation in north-eastern Germany. Quat. Int. 222, 72–79.
Lüttig, G., 1954. Alt- und mittelpleistozäne Eisrandlagen zwischen Harz und Weser. Geol. Jahrb. 70, 43–125.
Lüttig, G., 1958. Methodische Fragen der Geschiebeforschung. Geol. Jahrb. 75, 361–418.
Lüttig, G., 1960. Neue Ergebnisse quartärgeologischer Forschung im Raume Alfeld – Hameln – Elze. Geol. Jahrb. 77, 337–390.
Mahenke, V., Grosse, R., 1970. Beitrag zur Kenntnis des Pleistozäns nordwestlich von Leipzig. Geologie 19, 909–930.
Marks, L., 2011. Quaternary glaciations in Poland. In: Ehlers, J., Gibbard, P.L., Hughes, P.D. (Eds.), Quaternary Glaciations – Extent and Chronology – a Closer Look. Developments in Quaternary Science 15. Elsevier, Amsterdam, pp. 299–303.
Marks, L., Karabanov, A., Nitychoruk, J., Bahdasarau, M., Krzywicki, T., Majecka, A., Pochocka-Swarc, K., Rychel, J., Woronko, B., Zbucki, L., Hradunova, A., Hrychanik, M., Mamchyk, S., Rylova, T., Nowacki, L., Pielach, M., 2016. Revised limit of the Saalian ice sheet in central Europe. Quat. Int. https://doi.org/10.1016/j.quaint.2016.07.043.
Meijer, T., Cleveringa, P., 2009. Aminostratigraphy of middle and late Pleistocene deposits in The Netherlands and the southern part of the North Sea Basin. Glob. Planet. Change 68, 326–345.
Meinsen, J., Winsemann, J., Weitkamp, A., Landmeyer, N., Lenz, A., Dölling, A., 2011. Middle Pleistocene (Saalian) lake outburst floods in the Münsterland Embayment (NW Germany): impacts and magnitudes. Quat. Sci. Rev. 30, 2597–2625.
Meng, S., Wansa, S., 2008. Sedimente und Prozesse am Außenrand der Saale-Vereisung südwestlich von Halle (Saale). Z. Dtsch. Ges. für Geowiss. 159, 205–220.
Meyer, K.-D., 2005. Zur Stratigraphie des Saale-Glazials in Niedersachsen und zu Korrelationsversuchen mit Nachbargebieten. Eiszeitalt. Ggw. 55, 25–42.
Moreau, J., Huuse, M., Janszen, A., van der Vegt, P., Gibbard, P.L., Moscariello, A., 2012. The glaciogenic unconformity of the southern North Sea. In: Huuse, M., Redfern, J., Le Heron, D.P., Dixon, R.J., Moscariello, A., Craig, J. (Eds.), Glaciogenic Reservoirs. Geological Society of London, vol 368. Special Publication, pp. 99–110.
O'Connor, J.E., 1993. Hydrology, hydraulics, and geomorphology of the bonneville flood. Geol. Soc. Am. Special Pap. 274, 1–83.
Passchier, S., Laban, C., Mesdag, C.S., Rijsdijk, K.F., 2010. Subglacial bed conditions during Late Pleistocene glaciations and their impact on ice dynamics in the southern North Sea. Boreas 39, 633–647.
Penaud, A., Eynaud, F., Turon, J.L., Zaragosi, S., Malaizé, B., Toucanne, S., Bourillet, J.F., 2009. What forced the collapse of European ice sheets during the last two glacial periods (150ka BP and 18ka cal BP)? Palynological evidence. Palaeogeography, Palaeoclimatology. Palaeoecology 281, 66–78.
Perkins, A.J., Brennand, T.A., 2015. Refining the pattern and style of Cordilleran Ice Sheet retreat: palaeogeography, evolution and implications of lateglacial ice-dammed lake systems on the southern Fraser Plateau, British Columbia, Canada. Boreas 44, 319–342.
Pilger, A., Mocha, P., Petzold, B., Rösler, A., 1991. Die nordischen Gletscher am nordwestlichen Harzrand und ihre Stauseen. Clausthal. Geol. Abh. 48, 1–159.
Powell, R.D., 1990. Glacimarine processes at grounding-line fans and their growth to ice-contact deltas. In: Dowdeswell, J.A., Scourse, J.D. (Eds.), Glacimarine Environments: Processes and Sediments. Geological Society Special Publication 53. Geological Society, London, pp. 53–73.
Prescott, J.R., Hutton, J.T., 1994. Cosmic ray contributions to dose rates for luminescence and ESR dating: large depths and long-term time variations. Radiat. Meas. 23, 497–500.
Preusser, F., 1999. Lumineszenzdatierung fluviatiler Sedimente: fallbeispiele aus der Schweiz und Norddeutschland. Kölner Forum für Geol. Paläontol. 3, 63–63.
Reinecke, V., 2006. Untersuchungen zur jungpleistozänen Reliefentwicklung und Morphodynamik im nördlichen Harzvorland. Aachen. Geogr. Arb. 43, 1–170.
Roskosch, J., Winsemann, J., Polom, U., Brandes, C., Tsukamoto, S., Weitkamp, A.,

Bartholomäus, W.A., Henningsen, D., Frechen, M., 2015. Luminescence dating of ice-marginal deposits in northern Germany: evidence for repeated glaciations during the Middle Pleistocene (MIS 12 to MIS 6). Boreas 44, 103–126.
Ruske, R., 1961. Gliederung des Pleistozäns im Geiseltal und seiner Umgebung. Geologie 10, 152–168.
Ruske, R., 1963. Zur Entstehung des Gewässernetzes in der Umgebung von Halle/Saale. Hercynia NF. 1, 40–50.
Ruske, R., 1973. Stand der Erforschungen des Quartärs in den Bezirken Halle und Magdeburg. Z. für Geol. Wiss. 1, 1065–1086.
Ruske, R., Wünsche, M., 1964. Zur Gliederung des Pleistozäns im Raum der unteren Unstrut. Geologie 13, 211–222.
Salamon, T., Krzyszkowski, D., Kowalska, A., 2013. Development of Pleistocene glaciomarginal lake in the foreland of the Sudetes (SW Poland). Geomorphology 190, 1–15.
Saloustros, K., Speetzen, E., 1999. Aufbau und Genese der saalezeitlichen Grundmoräne bei Mittel-Gaupel im westlichen Münsterland (Westfalen, NW-Deutschland). Geol. und Paläontol. Westfalen 52, 41–49.
Schuberth, K., Radzinski, K.-H., 2014. Geologische Karte von Sachsen-Anhalt, 1: 25,000, Blatt 4635 Querfurt. Landesamt für Geologie und Bergwesen Sachsen-Anhalt, Halle.
Schulz, W., 1962. Gliederung der Pleistozänstratigraphie in der Umgebung von Halle (Saale). Geologie 36, 1–69.
Sejrup, H.P., Clark, C.D., Hjelstuen, B.O., 2016. Rapid ice sheet retreat triggered by ice stream debuttressing: evidence from the North Sea. Geology 44, 355–358.
Skupin, K., Zandstra, J.G., 2010. Gletscher der Saale-Kaltzeit am Niederrhein. Geologischer Dienst NRW, Krefeld, 117 pp.
Skupin, K., Speetzen, E., Zandstra, J.G., 1993. Die Eiszeit in Nordwestdeutschland. Zur Vereisung der Westfälischen Bucht und angrenzender Gebiete. Geologisches Landesamt Nordrhein-Westfalen, Krefeld, 143 pp.
Skupin, K., Speetzen, E., Zandstra, J.G., 2003. Die Eiszeit in Nordost-Westfalen und angrenzenden Gebieten Niedersachsens. Geologischer Dienst NRW, Krefeld, 95 pp.
Skupin, K., Speetzen, E., Zandstra, J.G., 2010. Früh-drenthezeitliche Moränen der Saale-Kaltzeit im Bereich der Abgrabung Tecklenborg südwestlich von Coesfeld-Flamschen (westliches Münsterland). Geol. und Paläontol. Westfalen 74, 69–87.
Speetzen, E., Wixforth, O., 2002. Geschiebeeinregelung und Gefügetypen am Beispiel saalezeitlicher Moränen im Münsterland und im Osnabrücker Land (NW-Deutschland). – Münstersche Forsch. zur Geol. Paläontol. 93, 139–157.
Speetzen, E., Zandstra, J.G., 2009. Elster-und Saale-Vereisung im Weser-Ems-Gebiet und ihre kristallinen Leitgeschiebegesellschaften. Münstersche Forsch. zur Geol. Paläontol. 103, 1–113.
Stephan, H.-J., 2014. Climato-stratigraphic subdivision of the Pleistocene in Schleswig-Holstein, Germany and adjoining areas. E&G Quat. Sci. J. 63, 3–18.
Stokes, C.R., Clark, C.D., 2003. The Dubawnt Lake palaeo-ice stream: evidence for dynamic ice sheet behaviour on the Canadian Shield and insights regarding the controls on ice-stream location and vigour. Boreas 32, 263–279.
Stokes, C.R., Clark, C.D., 2004. Evolution of late glacial ice-marginal lakes on the northwestern Canadian Shield and their influence on the location of the Dubawnt Lake palaeo-ice stream. Palaeogeography, Palaeoclimatology. Palaeoecology 215, 155–171.
Thiel, C., Buylaert, J.-P., Murray, A.S., Terhorst, B., Hofer, I., Tsukamoto, S., Frechen, M., 2011. Luminescence dating of the Stratzing loess profile (Austria) - testing the potential of an elevated temperature post-IR IRSL protocol. Quat. Int. 234, 23–31.
Thome, K.N., 1983. Gletscherерosion und -akkumulation im Münsterland und angrenzenden Gebieten. Neues Jahrb. für Geol. Paläontol. 166, 116–138.
Thomsen, K.J., Murray, A.S., Jain, M., Bøtter-Jensen, L., 2008. Laboratory fading rates of various luminescence signals from feldspar-rich sediment extracts. Radiat. Meas. 43, 1474–1486.
Toucanne, S., Zaragosi, S., Bourillet, J.F., Cremer, M., Eynaud, F., Vliet-Lanoë, Van, Penaud, A., Fontanier, C., Turon, J.L., Cortijo, E., Gibbard, P.L., 2009a. Timing of massive 'Fleuve Manche' discharges over the last 350kyr: insights into the European ice-sheet oscillations and the European drainage network from MIS 10 to 2. Quat. Sci. Rev. 28, 1238–1256.
Toucanne, S., Zaragosi, S., Bourillet, J.F., Gibbard, P.L., Eynaud, F., Giraudeau, J., Turon, J.L., Cremer, M., Cortijo, E., Martinez, P., Rossignol, L., 2009b. A 1.2 Ma record of glaciation and fluvial discharge from the West European Atlantic margin. Quat. Sci. Rev. 28, 2974–2981.
Van den Berg, M.W., Beets, D.J., 1987. Saalian glacial deposits and morphology in The Netherlands. In: van der Meer, J.J.M. (Ed.), Tills and Glaciotectonics. Balkema, Rotterdam, pp. 235–251.
Van der Vegt, P., Janszen, A., Moscariello, A., 2012. Tunnel valleys: current knowledge and future perspectives. In: Huuse, M., Redfern, J., Le Heron, D.P., Dixon, R.J., Moscariello, A., Craig, J. (Eds.), Glaciogenic Reservoirs. Geological Society of London, Special Publication, vol 368. Geological Society, London, pp. 75–97.
Van der Wateren, F.M., 1987. Structural geology and sedimentology of the Dammer Berge push moraine, FRG. In: Van der Meer, J.J.M. (Ed.), Tills and Glaciotectonics. A.A. Balkema, Rotterdam, pp. 157–182.
Waas, D., Kleinmann, A., Lepper, J., 2011. Uranium-thorium dating of peat horizons from pit Nachtigall in northern Germany. Quat. Int. 241, 111–124.
Wansa, S., 1997. Die Schotterterrassen der Saale und Salza nordwestlich von Halle. Leipz. Geowiss. 5, 135–149.
White, T.S., Bridgland, D.R., Westaway, R., Straw, A., 2017. Evidence for late Middle Pleistocene glaciation of the British margin of the southern North Sea. J. Quat. Sci. 32, 261–275.
Winsborrow, M.C., Clark, C.D., Stokes, C.R., 2010. What controls the location of ice streams? Earth Sci. Rev. 103, 45–59.
Winsemann, J., Asprion, U., Meyer, T., Schultz, H., Victor, P., 2003. Evidence of iceberg ploughing in a subaqueous ice-contact fan, glacial Lake Rinteln, NW Germany. Boreas 32, 386–398.
Winsemann, J., Asprion, U., Meyer, T., 2004. Sequence analysis of early Saalian glacial lake deposits (NW Germany): evidence of rapid ice margin retreat and associated calving processes. Sediment. Geol. 165, 223–251.
Winsemann, J., Asprion, U., Meyer, T., 2007a. Lake-level control on ice-margin subaqueous fans, glacial Lake Rinteln. In: Hambrey, M., Christoffersen, P., Glasser, N., Hubbard, B. (Eds.), Glacial Processes and Products. International Association of Sedimentologists Special Publication 39. Wiley, Chichester, pp. 121–148.
Winsemann, J., Asprion, U., Meyer, T., Schramm, C., 2007b. Facies characteristics of Middle Pleistocene (Saalian) ice-margin subaqueous fan and delta deposits, glacial Lake Leine, NW Germany. Sediment. Geol. 193, 105–129.
Winsemann, J., Hornung, J.J., Meinsen, J., Asprion, U., Polom, U., Brandes, C., Bußmann, M., Weber, C., 2009. Anatomy of a subaqueous ice-contact fan and delta complex, Middle Pleistocene, north-west Germany. Sedimentology 56, 1041–1076.
Winsemann, J., Brandes, C., Polom, U., 2011a. Response of a proglacial delta to rapid high-magnitude lake-level change: an integration of outcrop data and high-resolution shear-wave seismics. Basin Res. 23, 22–52.
Winsemann, J., Brandes, C., Polom, U., Weber, C., 2011b. Depositional architecture and palaeogeographic significance of Middle Pleistocene glaciolacustrine ice marginal deposits in northwestern Germany: a synoptic overview. E&G Quat. Sci. J. 60, 212–235.
Winsemann, J., Lang, J., Roskosch, J., Polom, U., Böhner, U., Brandes, C., Glotzbach, C., Frechen, M., 2015. Terrace styles and timing of terrace formation in the Weser and Leine valleys, northern Germany: Response of a fluvial system to climate change and glaciation. Quat. Sci. Rev. 123, 31–57.
Winsemann, J., Alho, P., Laamanen, L., Goseberg, N., Lang, J., Klostermann, J., 2016. Flow dynamics, sedimentation and erosion of glacial lake outburst floods along the Middle Pleistocene Scandinavian Ice Sheet (northern central Europe). Boreas 45, 260–283.
Winter, S., 1998. Petrographie und Interngefüge Drenthe-zeitlicher Grundmoränenkörper im niedersächsischen und sachsen-anhaltinischen Bergland zwischen Vlotho (Weser) und Hoym (nordöstliches Harzvorland). Universität Hannover unpublished diploma thesis, 70 pp.
Wintle, A.G., 1973. Anomalous fading of thermo-luminescence in mineral samples. Nature 245, 143–144.
Woldstedt, P., 1950. Norddeutschland und angrenzende Gebiete im Eiszeitalter. Koehler, Stuttgart, 464 pp.
Wolf, L., Alexowsky, W., Dietze, W., Hiller, A., Krbetschek, M., Lange, J.M., Seifert, M., Tröger, K.-A., Voigt, T., Walther, H., 1994. Fluviatile und glaziäre Ablagerungen am äußersten Rand der Elster-und Saale-Vereisung; die spättertiäre und quartäre Geschichte des sächsischen Elbgebietes (Exkursion A2). Altenbg. Naturwiss. Forsch. 7, 190–235.
Zandstra, J.G., 1987. Explanation to the map 'Fennoscandian crystalline erratics of Saalian age in The Netherlands'. In: Van der Meer, J.J.M. (Ed.), Tills and Glaciotectonics. Balkema, Rotterdam, pp. 127–132.